SPATIAL IMPACTS OF OFFSHORE WIND FARMS ON HYDRODYNAMICS AND BIOGEOCHEMICAL ENVIRONMENT

Scientific Report from DCE – Danish Centre for Environment and Energy No. 658 2025

AARHUS UNIVERSITY
DCE – DANISH CENTRE FOR ENVIRONMENT AND ENERGY

SPATIAL IMPACTS OF OFFSHORE WIND FARMS ON HYDRODYNAMICS AND BIOGEOCHEMICAL ENVIRONMENT

Scientific Report from DCE – Danish Centre for Environment and Energy No. 658 2025

Marie Maar
Vibe Schourup-Kristensen
Christian Mohn
Ange P. Ishimwe
Eva Friis Møller
Charlotte H. Clubley
Janus Larsen

Aarhus University, Department of Ecoscience

AARHUS UNIVERSITY
DCE – DANISH CENTRE FOR ENVIRONMENT AND ENERGY

Data sheet

Series title and no.:	Scientific Report from DCE – Danish Centre for Environment and Energy No. 658
Category:	Scientific advisory report
Title:	Spatial impacts of offshore wind farms on hydrodynamics and biogeochemical environment
Author(s):	Marie Maar[1], Vibe Schourup-Kristensen[1], Christian Mohn[1], Ange P. Ishimwe[1], Eva Friis Møller[1], Charlotte H. Clubley[1], Janus Larsen[1]
Institution(s):	Department of Ecoscience, Aarhus University[1]
Publisher:	Aarhus University, DCE – Danish Centre for Environment and Energy ©
URL:	http://dce.au.dk/en
Year of publication:	May 2025
Editing completed:	7. May 2025
Referee:	Lasse Tor Nielsen,
External referees, NIRAS:	Tony Bergøe and Rikke Holm
Quality assurance, DCE:	Anja Skjoldborg Hansen
Linguistic QA:	Charlotte Kler
External comments:	The comments can be found here:
Financial support:	Danish Energy Agency
Please cite as:	Marie Maar, Vibe Schourup-Kristensen, Christian Mohn, Ange P. Ishimwe, Eva Friis Møller, Charlotte H. Clubley, Janus Larsen. 2025. Spatial impacts of offshore wind farms on hydrodynamics and biogeochemical environment. Aarhus University, DCE – Danish Centre for Environment and Energy, 66 pp. Scientific Report No. 658
	Reproduction permitted provided the source is explicitly acknowledged
Abstract:	This report provides a model assessment of the spatial impact of current and future offshore wind development on hydrodynamics and the biogeochemical environment in the North Sea and the Inner Danish waters.
Keywords:	Spatial impacts, cumulative effects, offshore wind farms, hydrodynamics, biogeochemistry, stratification, primary production
Front page photo:	Colorbox
ISBN:	978-87-7156-953-7
ISSN (electronic):	2244-9981
Number of pages:	66

Content

Content 3

Preface 5

Sammenfatning 6

Summary 8

1 Introduction 10
- 1.1 Background 10
- 1.2 Model Scenarios 11

2 Description of the applied marine models 15
- 2.1 The North Sea model set-up 15
- 2.2 Inner Danish waters model set-up 18

3 Parameterization of offshore wind farm effects 20
- 3.1 Wind forcing 20
- 3.2 Drag effect of the monopiles 20
- 3.3 Stratification index 21

4 Sensitivity analysis of offshore wind 24
- 4.1 Ecosystem variables 24
- 4.2 Sensitivity analysis 24

5 Sensitivity to offshore wind in the North Sea 26
- 5.1 Ecosystem responses in the North Sea 26
  - Physical variables in the North Sea: 27
  - Biogeochemical variables in the North Sea: 29
- 5.2 Responses of PEA and primary production inside the offshore wind farms for Y2030 32
- 5.3 Spatial impact index for the North Sea and the Danish EEZ 34
  - PEA in the North Sea area: 34
  - PEA in the Danish EEZ: 34
  - Primary production in the whole North Sea: 35
  - Primary production in the Danish EEZ: 35
- 5.4 Extreme events 36

6 Sensitivity to offshore wind in the Inner Danish waters 38
- 6.1 Ecosystem responses of the Inner Danish waters 38
  - Physical variables in the Inner Danish waters: 38
  - Biogeochemical variables in the Inner Danish waters: 40
- 6.2 Responses of PEA and primary production inside the offshore wind farms for Y2030 43
- 6.3 Spatial impact index for the entire Inner Danish waters and the Danish EEZ 45

PEA for the entire model domain of Inner Danish waters: 45
Primary production for the entire model domain of the Inner Danish waters: 45
The Danish EEZ in the Kattegat and Arkona basin Y2030: 46
6.4 Extreme events 47

7 Model uncertainties 49

8 Discussion 51

9 References 54

10 Appendix A. Model validation and quality assurance 58
Validation of the applied models 58
10.1 Applied metrics 58
10.2 North Sea validation 58
10.3 North Sea physical and biogeochemical spatial patterns 60
10.4 Inner Danish waters validation 63
10.5 Inner Danish waters physical and biogeochemical spatial patterns 64
10.6 Model quality assurance 65

Preface

This report contributes to the project *"Environmental mapping and screening of the offshore wind potential in Denmark"* initiated in 2022 by the Danish Energy Agency. The project aims to support the long-term planning of offshore wind farms by providing a comprehensive overview of the combined offshore wind potential in Denmark. It is funded under the Finance Act 2022 through the programme "Investeringer i et fortsat grønnere Danmark" (Investing in the continuing greening of Denmark). The project is carried out by NIRAS, Danish Centre for Environment and Energy (DCE) - Aarhus University (Department of Ecoscience) and DTU Wind.

The overall project consists of four tasks defined by the Danish Energy Agency (https://ens.dk/energikilder/planlaegning-af-fremtidens-havvindmoelleparker):

1. Sensitivity mapping of nature, environmental, wind and hydrodynamic conditions.
2. Technical fine-screening and assessment of the overall offshore wind potential based on sensitivity mapping and relevant technical parameters.
3. Assessment of potential cumulative effects from large-scale offshore wind development in Denmark and neighbouring countries.
4. Assessment of barriers and potentials in relation to coexistence.

This report addresses one component of Task 1: sensitivity mapping and Task 3: Assessment of potential cumulative effects. Specifically, it provides an overview of offshore regions within the North Sea and inner Danish waters that shows an impact of current and potential future offshore wind farm development to hydrodynamics and biogeochemical environment using ecosystem modelling. The estimated spatial impact only considers two defined scenarios and not the sensitivity of all areas to offshore wind. Other subjects within Task 1- such as fish, marine mammals, bats, benthic habitats and wind - will be presented in separate reports in late 2024 and early 2025. A synthesis of all topics under Task 1 will be published in 2025.

The project management teams at both AU and NIRAS have contributed to the description of the background for the report and the relation to other activities in the preface. The report and the work contained within are solely the responsibility of the authors.

Sammenfatning

Denne rapport beskriver et modelstudie til vurdering af den rumlige påvirkning af nutidige og fremtidige havvindmølleparker på hydrodynamik og biogeokemiske miljøforhold i Nordsøen og de Indre Danske Farvande. Havvindmølleparkerne forventes at påvirke de fysiske og biogeokemiske miljøforhold via to mekanismer: reduktion af vindpåvirkning ved havoverfladen (wake effekt) og forøget vandmodstand omkring møllefundamenterne. Lavere vindpåvirkning forventes at lede til en mindre opblanding og en stærkere lagdeling af vandsøjlen. Omvendt vil en større vandmodstand forøge den lokale opblanding og reducere lagdelingen af vandsøjlen. En større opblanding kan give anledning til en vertikal transport af næringsstoffer til overfladevandet og stimulere primærproduktionen. En stærkere lagdeling vil på den anden side reducere næringsstoftilførslen fra bundlaget og potentielt begrænse primærproduktionen.

To modelscenarier blev evalueret for påvirkninger: i) den nuværende fordeling af havvindmølleparker (år 2021) og ii) den potentielle fremtidige fordeling af havvindmølleparker (år 2030) i forhold til et referencescenarie uden havvind i Nordsøen og de Indre Danske Farvande. Vi anvendte højkvalitets forceringsdata for vindpåvirkning, inklusiv realistiske fordelinger af havvindmøller og deres reelle størrelser, i 3D FlexSem modelsystemet. Den koblede hydrodynamiske - biogeokemiske model blev valideret mod moniteringsdata.

Blandt de testede økosystemvariable responderede lagdelingen af vandsøjlen, næringsstofkoncentrationer samt primærproduktionen stærkest på introduktionen af havvindmøller. I Nordsøen blev lagdelingen nedbrudt inde i vindmølleparkerne pga. en stærk opblanding omkring møllefundamenterne. I de Indre Danske Farvande blev lagdelingen forøget i et større område uden for havvindmølleparkerne på grund af wake effekten. I begge områder dominerede opblandingen omkring møllefundamenterne over wake effekten ved strømhastigheder over 0,15 m s^{-1}.

Primærproduktionen blev hovedsageligt forøget i og lige omkring havvindmølleparkerne i Nordsøen, mens der var en tendens til faldende værdier længere væk fra parkerne. I de Indre Danske Farvande viste primærproduktionen stor rumlig variation. Den faldt i nogle områder, mens den blev forøget i andre områder afhængig af ændringer i lagdelingen, men faldt generelt lidt i hele området. Den sæsonmæssige variation var størst inden for havvindmølleparkerne i forhold til hele modelområdet for Nordsøen og de Indre Danske farvande.

Det rumlige påvirkningsindeks (%, beregnet ud fra medianændringen i forhold til den naturlige variabilitet) viste en effekt både inden for og imellem havvindmølleparkerne, især i 2030 scenariet. Dette indikerer, at der er kumulative påvirkninger mellem naboparkerne i Danmark og andre lande i Nordsøen og i de Indre Danske farvande. I den danske eksklusive økonomiske zone var påvirkningerne under 20% i Nordsøen og 5% i de Indre Danske Farvande. Det rumlige indeks for den danske zone var generelt lavere end for de andre lande på grund af den lavere havvindmøllekapacitet og mindre tæthed af møllefundamenterne i de to scenarier samt de generelt lavere strømhastigheder.

Påvirkningsafstanden var generelt mindre end 5 km fra de danske havvindmøller i Nordsøen, dog med nogle mindre diffuse ændringer i områder mellem parkerne. I de Indre Danske Farvande var den rumlige påvirkning generelt mere diffus på grund af wake effekten, som påvirkede et større område, og ændringerne kunne ikke umiddelbart tilegnes en bestemt havvindmøllepark. Dette studie viser, at det er vigtigt at medtage både wake effekten og opblandingseffekten omkring møllefundamenterne i modelleringen, da de har modsatrettede påvirkninger. Dette giver et meget komplekst respons i tid og rum i marine områder.

Summary

This report provides a model assessment of the spatial impact of current and future offshore wind development on hydrodynamics and the biogeochemical environment in the North Sea and Inner Danish waters. Offshore wind farms are expected to influence the physical and biogeochemical environment through two mechanisms: decreased wind stress at the sea surface (wake effect) and increased friction (drag effect) around monopiles. A decrease in wind stress is expected to give less mixing and stronger stratification, whereas the monopile drag is expected to increase local mixing and reduce stratification of the water column. A higher mixing will transport more nutrients to the surface layer stimulating primary production, whereas stronger stratification will reduce the input of nutrients and limit primary production.

Two model scenarios evaluated the impact of i) current distribution and ii) potential future distribution in 2030 of offshore wind farms relative to a scenario without wind farms in the North Sea and the Inner Danish waters. We applied high quality forcing data for the wind wakes, including realistic wind farm distribution and real turbine size in the 3D FlexSem model system. The coupled hydrodynamic-biogeochemical models were validated against monitoring data.

Stratification of the water column, nutrient concentrations and primary production responded most strongly to offshore wind among the considered variables in both areas. Stratification decreased in the offshore wind farm areas in the North Sea due to strong monopile mixing. In the Inner Danish waters, stratification increased in a larger area outside the offshore wind farms due to the wind wake effect. The monopile mixing effect was found to dominate over the wind wake effect at water current speeds >0.15 m s^{-1} in both areas.

Primary production mainly increased in the offshore wind farm areas in the North Sea, but decreased outside - although to a lesser degree. In the Inner Danish waters, primary production showed a high spatial variability with both decreasing and increasing values due to changes in stratification. Overall, primary production decreased slightly in the Inner Danish waters. The seasonal variability was highest inside the offshore wind farm areas compared to the model domain in both the North Sea and the Inner Danish waters.

The spatial impact index (%, estimated as the median response relative to the natural variability) showed that the effects extended outside the offshore wind farms, especially in the year 2030 scenario, indicating cumulative effects from neighboring farms in Denmark and other countries in both the North Sea and the Inner Danish waters. For the Danish EEZ, the spatial impact index was <20% in the North Sea and <5% in the Inner Danish waters. The spatial impact index for the Danish EEZ was generally lower than in the neighboring countries due to lower wind farm capacity and lower monopile density in the two scenarios and generally lower current speeds.

The impact range was generally less than 5 km from the Danish wind farms in the North Sea, although there were some smooth gradients between wind farms. In the Inner Danish waters, the spatial impacts were more diffuse due to the wind wake affecting a larger area and changes cannot be assigned to a specific wind park. The present study shows the importance of including both the wind wake effect and the monopile drag effect in the modelling since they are opposing forces, making the responses highly complex in space and time in marine waters.

1 Introduction

1.1 Background

Offshore wind farms are expected to influence the physical and biogeochemical environment through two mechanisms: changes in wind stress at the sea surface (wake effect) and increased friction (drag effect) around monopiles (Figure 1.1). Offshore wind farms extract kinetic energy from the atmospheric flow, which reduces the wind speed in their wake (Volker et al. 2017). The wake effect causes a reduced wind stress at the sea surface and can e.g. lead to less turbulent mixing, change current circulation, form dipoles of sea surface height, change stratification intensity and pattern and reduce bottom stress (Christiansen et al. 2022). The second mechanism is increased friction and turbulence from the monopiles, leading to more local turbulent mixing of the water column and changes in current speed (Rennau et al. 2012, Christiansen et al. 2023). Hence, the two mechanisms, wind wakes and drag effect, counteract each other with respect to the mixing/stratification of the water column (Christiansen et al. 2023). Previous studies have shown that the observed effects not only occur inside the wind farms, but also on a regional scale many kilometers away (Li et al. 2014, Cazenave et al. 2016, Schultze et al. 2020, Lu et al. 2022). The combined effect of wind wakes and monopile drag on hydrodynamics is therefore a complex interaction, both spatially and temporally, depending on the environmental conditions. To this end, 3D numerical modelling of hydrodynamics combined validated against *in situ* measurements is a powerful tool that can be used to assess the overall impacts of offshore windfarm development on marine ecosystems.

Changes in the hydrodynamics can influence the spatial-temporal distribution of e.g. temperature, salinity, nutrients, phytoplankton and oxygen potentially, leading to changes in the ecological state and productivity of marine ecosystems (Daewel et al. 2022). In the Baltic Sea, a model study showed that expansion of wind power would cause a shallowed halocline and increased deep water salinities (Arneborg et al. 2024). In the North Sea, mixing by monopile drag was suggested to cool the surface layer, whereas the wind wake would cause a warming effect during the stratified summer season (Christiansen et al. 2023). The same model (without monopile drag) showed that wind wakes changed primary production ±10% both inside and outside the windfarms, increased sediment content in the deeper areas, and reduced oxygen concentrations in deep waters (Daewel et al. 2022). Another model study showed a delay of the stratification and onset of the spring bloom in the southern central North Sea due to increased mixing by the monopiles (van Duren et al. 2021).

Overall, changes in the physical and biogeochemical patterns may have effects on marine life in terms of changes in the timing and availability of food and habitat suitability. However, the simulated changes rely on the model parameterizations of the large-scale wind farm development that vary between studies (Table 1.1). In the present study, we evaluated the impact of current distribution and potential future distribution in 2030 of offshore wind farm in the North Sea and the Inner Danish waters using the FlexSem model system. We applied high quality forcing data for the wind wakes and monopile drag, including realistic wind farm distribution and real turbine size in the 3D coupled hydrodynamic-biogeochemical model. Previous studies either applied more simple formulations of the wind wake, did not include monopile mixing, or did not consider the biogeochemistry (Table 1.1).

Table 1.1. Examples of large-scale offshore wind farm model studies for the North Sea and Baltic Sea and if/how they included wind wake and monopile drag effects in the model.

Area	Hydrodynamic model	Wind wakes	Monopile drag	Biogeochemistry	Reference
North Sea-Inner DK waters	FlexSem	Interactive atmospheric model with realistic wind farm distribution and real turbine sizes	yes	yes	Present study
Baltic Sea	NEMO-NORDIC	Max. 8% reduction of wind speed and exp. decay function	yes	no	Arneborg et al. 2024
North Sea	ECOSMO	Interactive atmospheric model with realistic wind farm distribution, single type turbine	no	no	Christiansen et al. 2022
German Bight	ECOSMO	Max. 8% reduction of wind speed and exp. decay function	yes	no	Christiansen et al. 2023
North Sea	ECOSMO	Interactive atmospheric model with realistic wind farm distribution, single type turbine	no	yes	Daewel et al. 2022
North Sea	3D-DCSM-FM	Constant 10% reduction of wind speed inside wind farms, no wake effect	yes	yes	van Duren et al. 2021

1.2 Model Scenarios

In the present study, the response of the marine physical and biogeochemical environment to offshore wind farm development was tested by running three scenarios using 3D coupled hydrodynamic-biogeochemical models for the North Sea and the Inner Danish waters. The meteorological year 2019 was chosen as a typical year over the last 30 years according to wind speed, wind direction and atmospheric stability distributions (Hahmann et al. 2025). The meteorological forcing described changes in wind speed and direction, air temperature, cloud cover and specific humidity.

The wind farm scenarios were developed by the Danish Energy Agency and DTU WIND and consisted of i) a reference scenario with no wind turbines on land and offshore (REF-NO-FARM), ii) current situation in 2021

(CURRENT) and iii) future scenario for 2030 (Y2030) (Table 1.2, Figure 1.2). The offshore wind farm capacity was 24.4 GW in CURRENT and 218.0 GW in Y2030, while the onshore wind farm capacity was 50.4 GW in both scenarios. The scenarios are described in more detail in Hahmann et al. (2025) and reports by the Energy Agency (Energistyrelsen 2024a, b).

The mean changes in wind speed (April to October 2019, relative to the reference scenario) were highest in Y2030 compared to CURRENT due to the higher wind farm capacity. In the North Sea, mean changes in wind speeds were higher compared to the Inner Danish Waters due to the higher wind farm capacity (Figure 1.3). In some areas, there was a small increase in wind speed in both CURRENT and Y2030 relative to the reference scenario, e.g. in the central part of the North Sea and the south-eastern part of the Inner Danish Waters at the Oder Lagoon. This was due to compensating mechanisms in the atmosphere (Hahmann et al. 2025).

Two short-term extreme periods in 2019, representing weak and strong wind wake effects, were selected for a more detailed analysis (Table 1.2). The first case (CALM) represented minimal wake effects during periods with wind speeds < 5 m s^{-1}, as most turbines generate only weak thrust force at wind speeds below 5 m s^{-1} (turbine cut-in wind speed). The second case (WINDY) was chosen to simulate strong and extensive wind farm wakes with stable atmospheric conditions. The results from both cases were compared as differences to the reference scenario (no wind farms). Possible effects on stratification (expressed as the potential energy anomaly) were analyzed in two future wind farm areas: One in the eastern North Sea, and another in the eastern Belt Sea, west of Bornholm.

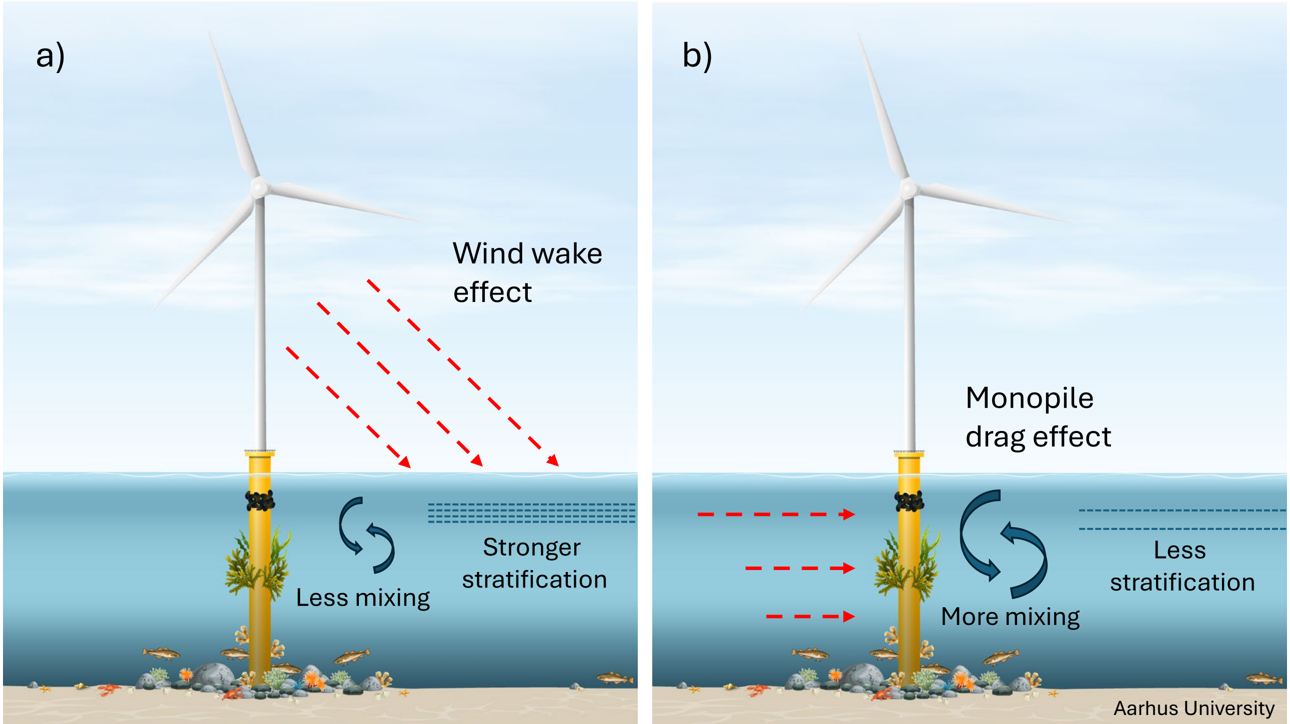

Figure 1.1.a) The wind wake causes reduced wind stress at the sea surface, less mixing and stronger stratification of the water column. b) The drag effect from monopiles causes increased local mixing and less stratification of the water column. Hence, the two effects from offshore wind are causing opposite effects on water column mixing and stratification operating on different temporal-spatial scales.

Table 1.2. Scenarios used in the FlexSem simulations. The onshore wind farm capacity was 50.4 GW in CURRENT and Y2030 scenarios.

Simulation	Wind farm scenario	Meteorological year	Offshore wind farm capacity (GW)
Scenarios			
REF-NO-FARM	No wind farms	2019	-
CURRENT	Wind farms as of November 2021	2019	24.4
Y2030	Wind farm scenario 2030	2019	218
Extreme events			
CALM	Wind speeds below 5m s^{-1} in Y2030 (2 days in May, 2 days in July)	2019	218
WINDY	Very stable atmospheric conditions with wind speeds around highest turbine thrust coefficients in Y2030 (5 days in April, 4 days in May, 14 days in June, 10 days in July)	2019	218

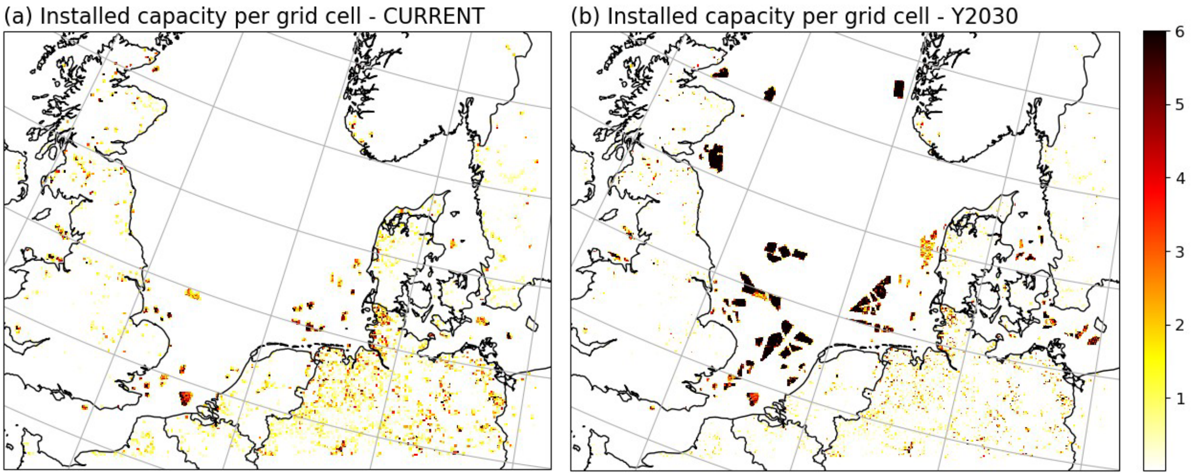

Figure 1.2. Installed wind farm capacity (MW km^{-2}) in the Weather Research and Forecasting (WRF) model in the a) CURRENT and b) Y2030 scenarios. From Hahmann et al. (2025).

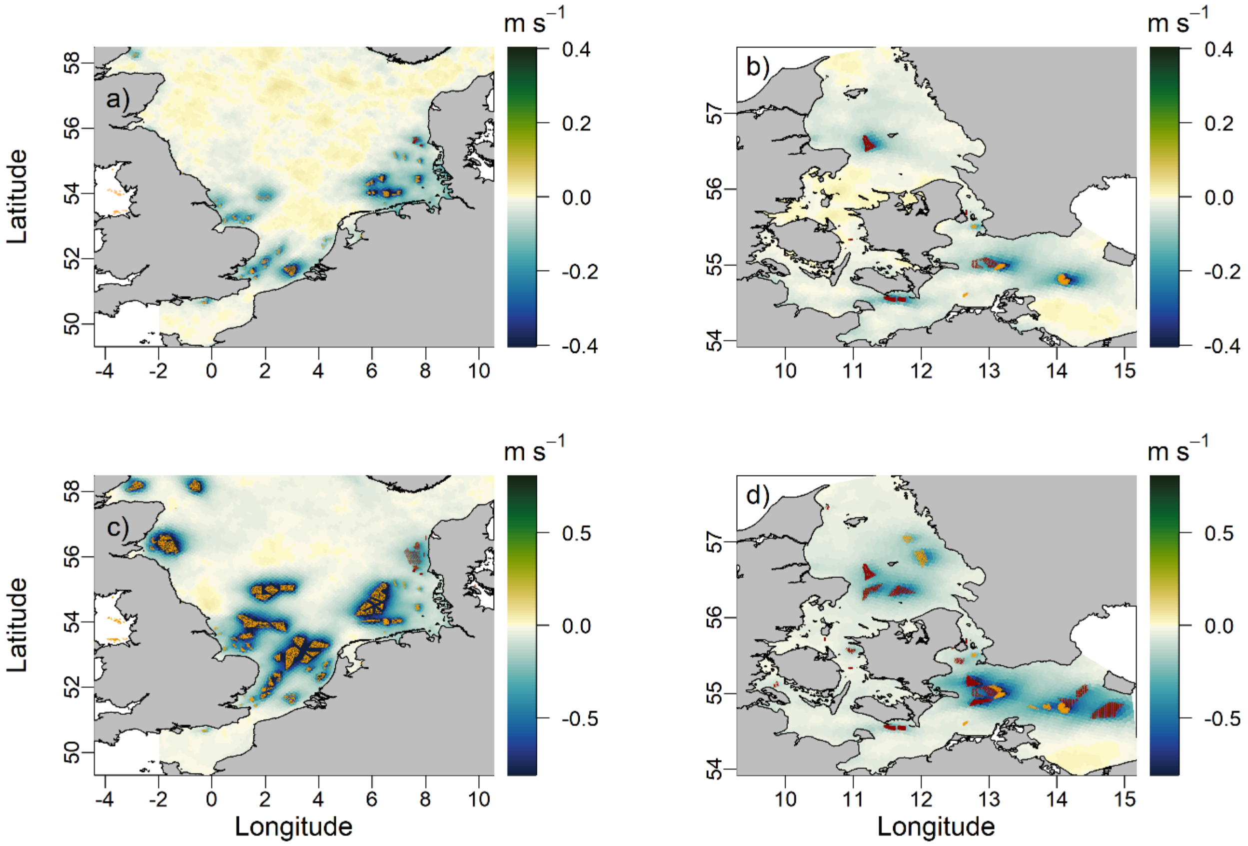

Figure 1.3. Difference in mean wind speed (m s^{-1}) between CURRENT and REF-NO-FARM in a) the North sea and b) Inner Danish waters, and between Y2030 and REF-NO-FARM for c) the North Sea and d) the Inner Danish Waters. The Danish offshore wind farms are shown as red points and other wind farms as orange points. Note the different scales.

2 Description of the applied marine models

2.1 The North Sea model set-up

A high-resolution hydrodynamic modelling system was applied for the entire North Sea using the open source FlexSem modelling framework (Larsen et al. 2020, Schourup-Kristensen et al. 2024) (https://marweb.bios.au.dk/Flexsem/). The hydrodynamic model provides values for e.g. salinity, temperature, current velocity and water mixing for all points in the model domain. FlexSem is a coastal 3-dimensional hydrodynamical model that solves the standard Navier-Stokes equations under the Boussinesq approximation. The Boussinesq approximation is used in most hydrodynamic models to simplify buoyancy driven flows in the Navier Stokes equations of motion. The time-step was 2 minutes. To reproduce the tidal environment of the North Sea, wetting and drying have been incorporated into the current setup of FlexSem. The model area covers the Greater North Sea (OSPAR region II), extending from the English Channel in the south to the northern North Sea/Norwegian Trench in the north and to the Skagerrak in the north-east (Figure 2.1).

FlexSem applies numerical techniques to increase the horizontal and vertical resolution in areas of specific interest. Grid refinement in these areas is provided using an unstructured computational mesh covering the entire range from platforms to basin scale. The horizontal resolution of the computational mesh varies from 7.8 km in the central North Sea, 3.9 km in the western North Sea and coastal areas to 2.5 km in the Wadden Sea. The vertical resolution consists of 10 layers of 5 m thickness, five layers of 10 m thickness, five layers of 20 m thickness, and nine layers of 50 m thickness (in total 29 layers) with a maximum depth of 682 m in the Norwegian Trench. The computational mesh consists of 12,721 polygons, 121,474 computational cells, and the model area is 484,087 km^2.

The turbulent part of the hydrodynamic solution was modeled by a *k*-epsilon model in the vertical (Burchard et al. 1998, Warner et al. 2005) and a Smagorinsky model in the horizontal (Smagorinsky 1963). A surface radiation model was added to the setup, which calculated the heat transfer through the ocean surface and modified the water temperature by calculating the short-wave radiation, the long-wave radiation, the sensible heat flux, and the latent heat flux (heat evaporation). The latter three are surface layer effects, whereas the short-wave radiation penetrates the surface and attenuates throughout the upper water column (Larsen et al. 2020). Evaporation does not affect salinity in the model. Initial and open boundary data was obtained from "CMEMS North-West European Shelf Ocean forecasting system" (Crocker et al. 2020), which can be downloaded at Copernicus E.U. Copernicus Marine Services.

Daily riverine inputs from the 18 Danish sources were obtained from the Danish national monitoring program NOVANA (Windolf et al. 2011). The OSPAR ICG-EMO riverine database of European rivers provided data for the other countries (Germany, United Kingdom (UK), the Netherlands, Belgium, France, and Norway). The ICG-EMO database contains daily values for discharge rates and nutrients for 368 rivers along the European Shelf, following optimization to daily values from originally sourced observational data (Lenhart et al. 2010, van Leeuwen et al. 2023). Please note that the riverine data for the UK has not been formally checked or authorized by the UK and that any conclusions drawn from it need to be treated with caution. Total-N is distributed into 90% NO_3, 2% NH_4 and 8% detritus and Total-P was assumed to 48% PO_4 based on monitoring data from streams (Maar et al. 2016).

The hydrodynamic model was coupled to a biogeochemical model simulating the cycling of nitrogen (N) and phosphorous (P) using Redfield ratios (Maar et al. 2011, Maar et al. 2016, Maar et al. 2022). The 10 state variables describe concentrations of inorganic nutrients (NO_3, NH_4, PO_4), two functional groups of phytoplankton (diatoms, flagellates), micro- and mesozooplankton, detritus, oxygen, and suspension feeders (Figure 2.2). The model considers the processes of nutrient uptake, growth, grazing, respiration, excretion, recycling, mortality and settling of detritus and diatoms (Maar et al. 2018). Chl *a* concentrations are used as a proxy for phytoplankton biomass using a conversion factor of 2 mg Chl *a* (mmol-N)$^{-1}$ (Thomas et al. 1992).

The pelagic model is two-way coupled to a sediment biogeochemical model through sedimentation of organic matter and diffusive fluxes of nutrients and oxygen. Pelagic detritus and diatoms settle into an organic detritus pool and a dead diatom pool, respectively, in the unconsolidated top layer of the sediment. Organic matter in the unconsolidated sediment can be resuspended, ingested, respired, recycled or gradually transferred to the consolidated sediment layer as a first order process. In the consolidated layer, organic matter is slowly respired, recycled or buried if values >4500 mmol m^{-3}. Recycled nutrients in the sediment porewater are exchanged with the bottom water through diffusion. A fraction of the recycled NO_3 is lost in the denitrification process. Under oxidized conditions, PO_4 is retained in the sediment by adsorption to metals and released when the sediment becomes reduced. Benthic suspension feeders ingest phytoplankton and detritus, whereas deposit feeders ingest freshly deposited diatoms and detritus in the consolidated sediment.

Initial and open boundary data for the biogeochemical model was obtained from the Atlantic- European North West Shelf- Ocean Biogeochemistry Reanalysis (Ciavatta et al. 2018) and the Baltic Sea Biogeochemistry Reanalysis (https://doi.org/10.48670/moi-00012). There was a spin-up of one year to get semi-equibrilium status of the water column and three years for the sediment. Model validation is presented in Appendix A.

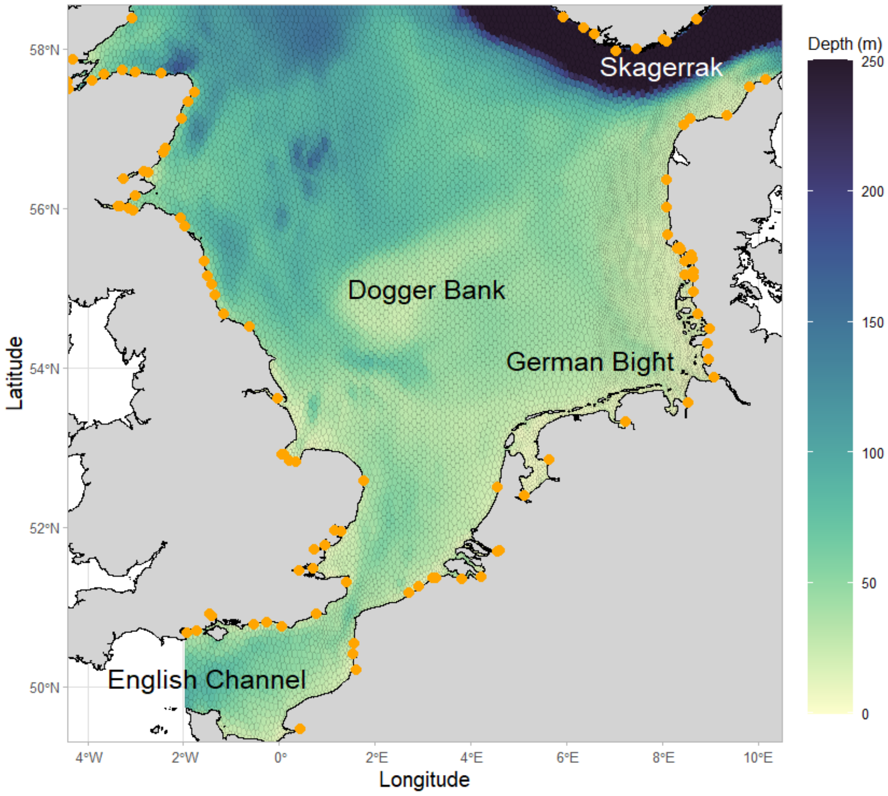

Figure 2.1. The North Sea model domain showing the bathymetry (color bar), model mesh (polygons) as well as position of freshwater sources (dots) (maximum depth is 680 m in the Skagerrak).

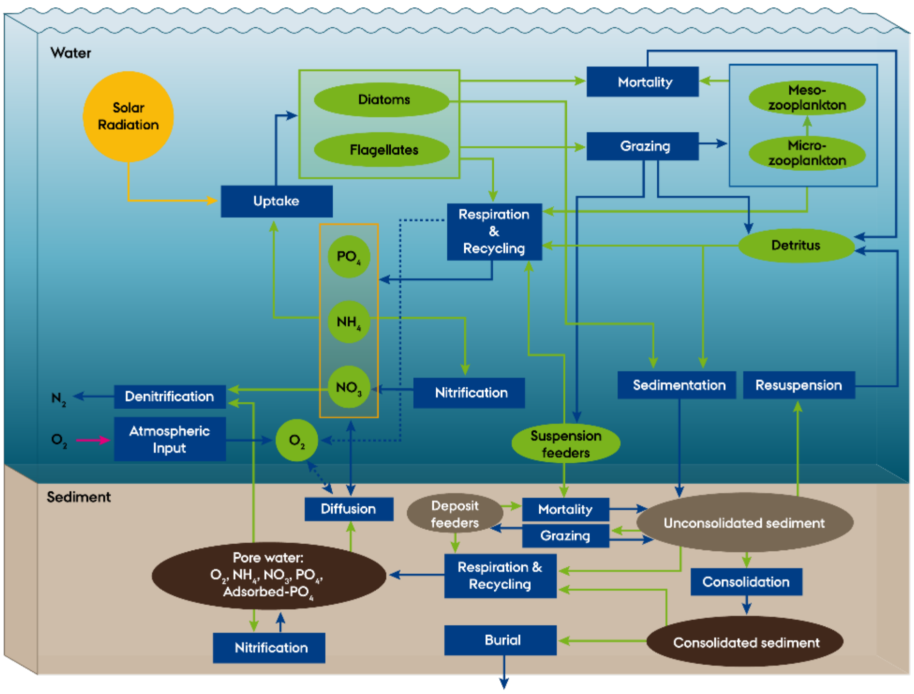

Figure 2.2. The applied biogeochemical model in FlexSem showing pelagic and sediment state variables in green and brown ovals, respectively, and processes in blue boxes.

2.2 Inner Danish waters model set-up

A high-resolution hydrodynamic modelling system was applied for the Inner Danish waters using the open source FlexSem modelling framework (Larsen et al. 2020, Larsen 2024), see description for the North Sea model (https://marweb.bios.au.dk/Flexsem/). The time-step was 1.5 minutes. The model domain for the inner Danish waters (Figure 2.3) was discretized into unstructured polygons in the horizontal, while the vertical discretization was carried out on a stratified grid. The horizontal resolution ranged from approximately 200 meters in the Little Belt, to 5 km in northern Kattegat and the western Baltic Sea. In the vertical, the mesh had a resolution of 1 meter and 84 layers. The surface layer had a thickness of 2 meters to allow fluctuations in sea surface height and the maximum depth was 84.5 meters. The computational mesh consisted of 11,244 polygons, 216,981 computational cells, and the model area was 66,369 km^2.

Boundary conditions for temperature, salinity, sea surface height, and velocities were provided by the Baltic Sea Physics Analysis and Forecast made available by SMHI and the E.U Copernicus Marine Service Information (https://doi.org/10.48670/moi-00010). For Danish coastlines, data for daily freshwater and nutrient runoff was obtained from the DK-QNP model (Windolf et al. 2011). For Swedish and German coastlines, these came from the E-HYPE catchment model (Lindström et al. 2010).

The biological model applied for the North Sea was here updated with two classes of dissolved organic nitrogen for the simulation, one labile class with a faster turnover rate and one refractory class with a slower turnover rate based on the ERGOM model for the Baltic Sea (Neumann et al. 2022). Initial values and boundary conditions for nitrate, ammonium, phosphate and oxygen were taken from a NEMO-ERGOM setup of the Baltic Sea (E.U. Copernicus Marine Services, https://doi.org/10.48670/moi-00012). For DON, boundary conditions were obtained from observational stations in the Kattegat and the Arkona Basin (www.odaforalle.au.dk). Aeolian deposition of nitrogen was assumed to be constant across the model domain, with a value of 13.4 mg-N m^{-2} $year^{-1}$ (Svendsen & Tornbjerg 2022). Model validation is presented in Appendix A.

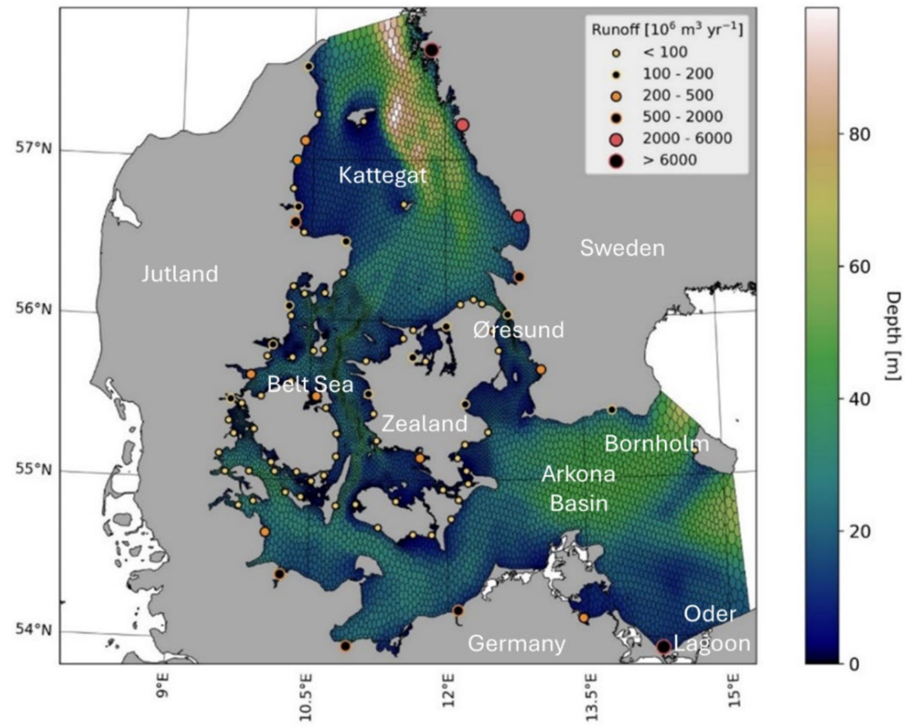

Figure 2.3. The Inner Danish waters model domain showing the bathymetry (color bar), model mesh (polygons) as well as position and strength of freshwater sources (dots).

3 Parameterization of offshore wind farm effects

3.1 Wind forcing

The meteorological forcing (wind, air temperature, cloud cover, specific humidity) at the sea surface came from the high-resolution Weather Research and Forecasting (WRF) model provided by DTU WIND (Hahmann et al. 2025). The WRF model was modified to generate the wake effects of offshore and onshore wind farms in the scenarios CURRENT and Y2030. The WRF model and scenarios are described in more detail in Hahmann et al. (2025).

The wind stress at the sea surface was described as (Smith & Banke 1975):

$$\tau = \rho_a \left(C_0 + C_1 u\right) u^2 \qquad \text{(eq. 1)}$$

where the wind drag coefficient is a linear function of the difference between the wind speed and the water current speed (u) and ρ_a is the density of the atmosphere. The values of the coefficients (C_o and C_1) can be found in Smith and Banke (1975). This formulation allows us to better consider weak and intense winds with, respectively, the first and second coefficients.

3.2 Drag effect of the monopiles

Offshore monopiles providing foundations for marine wind turbines constitute physical obstacles for the ocean currents. The drag provided by the monopiles slows down the mean currents and generates increased turbulence in the wake of the currents. The increased turbulence causes increased horizontal and vertical mixing in the vicinity of the monopile, which is advected by the currents into the surrounding region, which, again, affects the biogeochemistry and primary production (van Duren et al. 2021).

The physical effects of monopiles can be modelled by a model in sufficiently high resolution to resolve the monopile as an 'island' in the water. The drawback of this method is very high computational cost, particularly for a larger area with many monopiles like the North Sea. Alternatively, the processes can be parameterized by adding drag and turbulent kinetic energy in a coarser model (Rennau et al. 2012). This method is computationally effective, as it does not require very high resolution. The parameterization is dependent on the ocean state and not well validated, as direct measurements of the effects are difficult, expensive and, therefore, sparse (Christiansen et al. 2023).

In this study, we have chosen the parameterization method suggested by Rennau et al. (2012). The parameterization estimates the drag as:

$$F = \frac{1}{2} C_d \rho_0 d \vec{u} |\vec{u}| \qquad \text{(eq. 2)}$$

where C_d is the drag coefficient, ρ_0 the water density, d the diameter of the monopile and u the water velocity. The additional turbulent energy was estimated as:

$$P = \frac{1}{2} C_d a (u^2 + v^2)^{2/3} \qquad \text{(eq. 3)}$$

where a is the area density of the monopiles and u and v the current velocity components. The monopile diameter was assumed to be 7.5 m for turbines <15 MW and 13 m for turbines ≥15 MW in both offshore wind farm scenarios.

In the FlexSem setups for the North Sea and Inner Danish Waters, the drag coefficient is set to 0.63 as suggested by Rennau et al. (2012). This coefficient is uncertain and is dependent on the physical shape of the monopile, particularly growth on the monopile, such as mussels or seaweed. The diffusion coefficient is chosen to be 1.4, representing a "weak mixing" scenario (Rennau et al. 2012), but this is also subject to uncertainty, and values between 0.6 and 1.4 have been suggested by Christiansen et al. (2023). The results from a high-resolution FlexSem flume proof-of-concept model demonstrated good agreement between a configuration with an existing monopile featuring the monopile drag parameterization and measurements of the currents downstream of the monopile (Mohn et al. 2025).

3.3 Stratification index

The water column can be stratified due to differences in salinity and/or temperature and thereby limit the vertical exchange of nutrients and oxygen that is important for the biogeochemical processes. Stratification is expected to be impacted by offshore wind farm development. The wake effect causes reduced wind stress at the sea surface and stronger stratification, whereas the drag effect from monopiles causes increased local mixing of the water column (Figure 1.1).

The stratification index was estimated as the Potential Energy Anomaly (PEA, J m^{-3}), indicating the amount of energy needed to mix the water column (Simpson & Bowers 1981).

$$PEA = \frac{1}{H} \int_{-H}^{0} gz(\bar{\rho} - \rho)\, dz \qquad \text{(eq. 4)}$$

where H is water depth (m), g is the gravitational acceleration (m s^{-2}), z is the depth layer (m) in the water column, ρ is water density (kg m^{-3}) and $\bar{\rho}$ is the average density (kg m^{-3}) of the column estimated as:

$$\bar{\rho} = \frac{1}{H} \int_{-H}^{0} \rho\, dz \qquad \text{(eq. 5)}$$

The water column was considered mixed at PEA<10 J m^{-3} in the North Sea and gradually more stratified with increasing PEA values (van Leeuwen et al. 2015, Christiansen et al. 2023). On average, the seasonal development of stratification begins in April and lasts until October in the North Sea (Figure 3.1a). In the Inner Danish waters, the water column is generally more stratified than in the North Sea due to salinity stratification (Figure 3.1b). During summer, the temperature stratification also contributes to the stratification. The water column was considered mixed or weakly stratified at PEA<50 J m^{-3} in the Inner Danish waters and gradually more stratified with increasing PEA values.

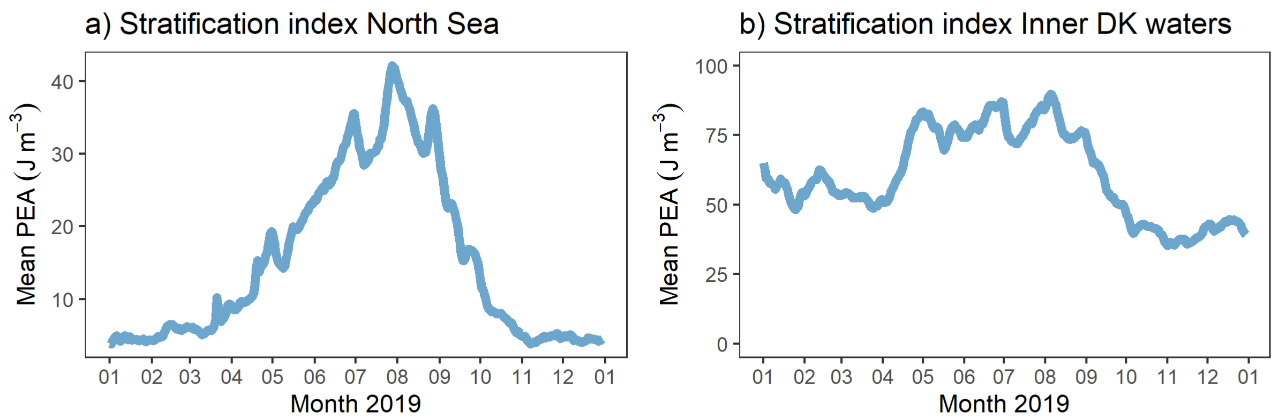

Figure 3.1. Time series of seasonal stratification index as means for the whole a) North Sea and b) Inner Danish waters 2019 from the REF-NO-FARM scenario.

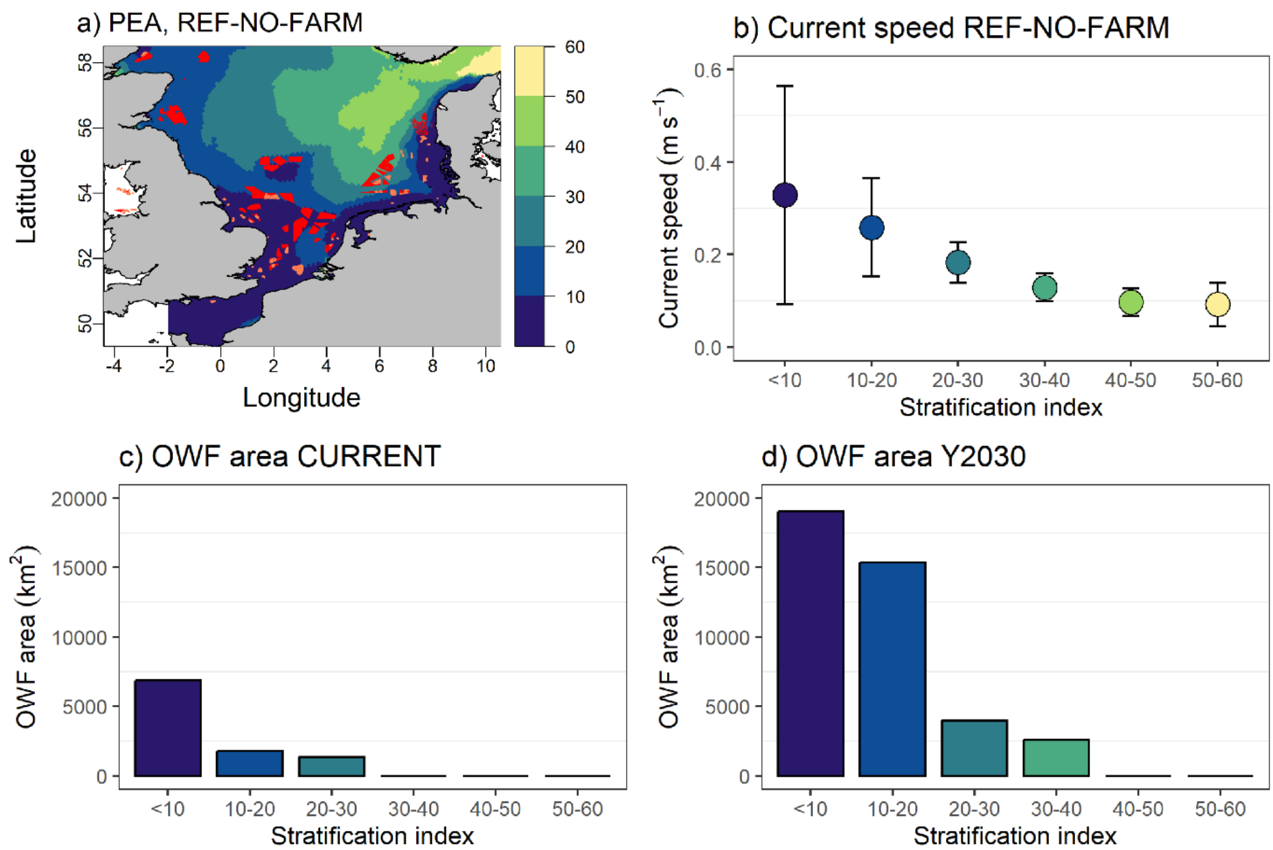

Figure 3.2. a) Spatial stratification index (PEA) and b) surface mean (±std) current speed (m s^{-1}) in the REF-NO-FARM scenario from April to October 2019 in the North Sea. Model area (km^2) covered by wind farms in c) CURRENT and d) Y2030 for different intervals of PEA. The wind farms in a) are indicated as orange and red points for CURRENT and Y2030, respectively. Note that the color bars represent PEA intervals shown on the map in a).

In the North Sea, the southern tidal and coastal areas were mostly mixed (PEA<10 J m^{-3}), and stratification increased towards Skagerrak in the northeast (Figure 3.2a). Surface current speed was highest in the mixed areas and decreased gradually with increasing PEA (Figure 3.2.b). The model area covered by offshore wind farms in CURRENT was highest in mixed areas, whereas the 2030 scenario showed an extension into more stratified areas (Figure 3.2c). In Y2030, there was an almost equally areal distribution between mixed areas and more stratified areas (>10 J m^{-3}) (Figure 3.2d).

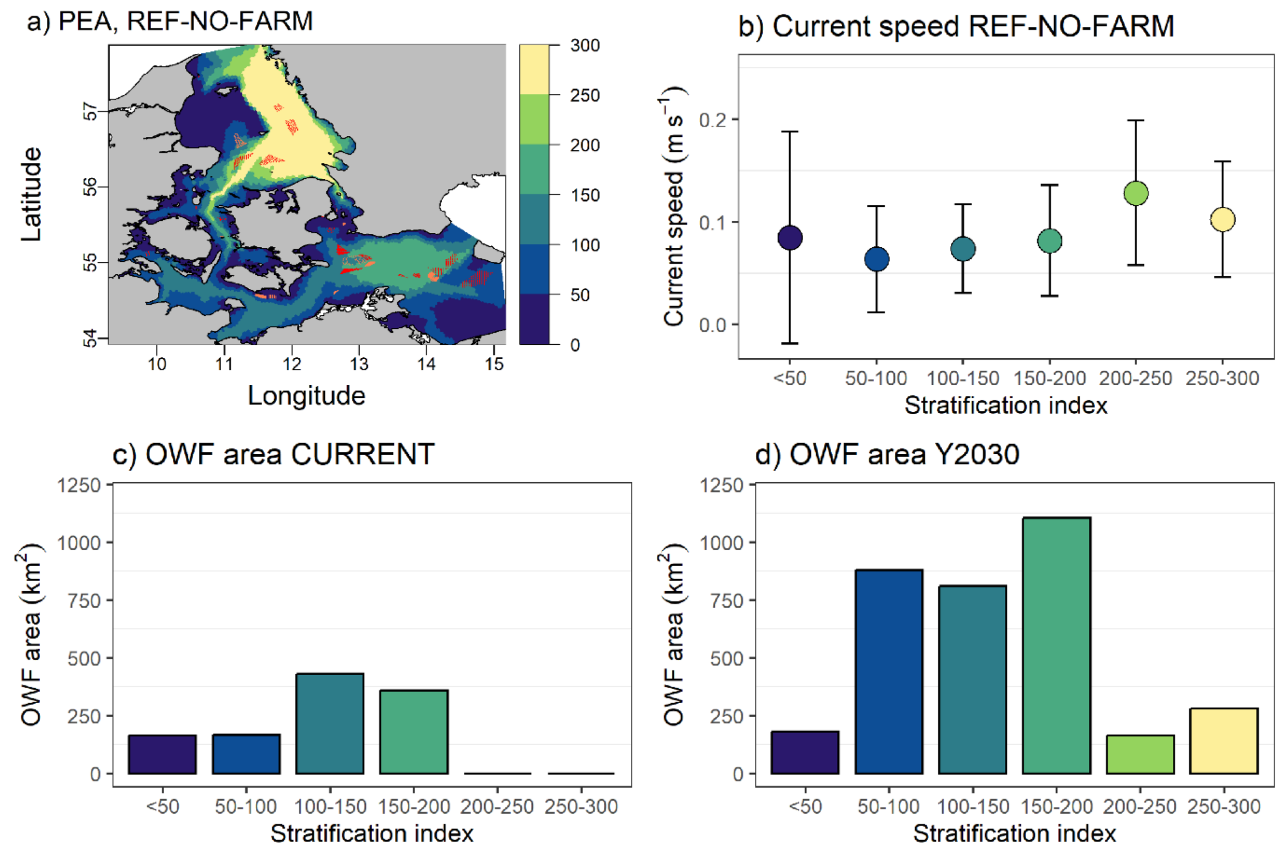

Figure 3.3. a) Spatial stratification index (PEA) and b) surface mean (±std) current speed (m s^{-1}) in the REF-NO-FARM scenario from April to October 2019 in the Inner Danish waters. Model area (km^2) covered by wind farms in c) CURRENT and d) Y2030 for different intervals of PEA. The wind farms in a) are indicated as orange and red points for CURRENT and Y2030, respectively. Note that the color bars represent PEA intervals shown on the map in a).

In the Inner Danish waters, the shallow coastal areas were mostly mixed or weakly stratified (PEA<50 J m^{-3}), and stratification increased towards the Great Belt, eastern Kattegat and the Arkona basin (Figure 3.3a). Surface current speed was highest in the mixed areas and the strongly stratified areas, with PEA>200 J m^{-3} (Figure 3.3b). In comparison, the mean current speed was lower than for the tidal areas in the North Sea. The model area covered by offshore wind farms in CURRENT was highest in stratified areas, with PEA from 100-200 J m^{-3}, whereas the 2030 scenario showed the highest development at PEA 50-200 J m^{-3}, with smaller extension into strongly stratified areas (Figure 3.3c, d).

4 Sensitivity analysis of offshore wind

4.1 Ecosystem variables

The sensitivity analysis of the large-scale offshore wind farm development was based on model results from the FlexSem 3D hydrodynamic-biogeochemical model applied to the North Sea and the Inner Danish waters. The selected ecosystem variables were stratification index (PEA), surface current speed, bottom stress, surface temperature, surface salinity, light attenuation (Kd), surface nutrient concentrations (nitrate and phosphate), surface Chlorophyl *a* (Chl *a* as a proxy for phytoplankton biomass), depth-integrated primary production and zooplankton production, zooplankton biomass, bottom oxygen and benthos biomass (Table 4.1).

Table 4.1. Overview of the considered ecosystem variables in the sensitivity analysis. NS=North Sea, IDW=Inner Danish Waters.

Physical variables	Units	Biogeochemical variables	Units
Stratification index (PEA, 0-40 m NS, 0-20 m IDW)	J m^{-3}	Surface nitrate	mmol-N m^{-3}
Surface current speed	m s^{-1}	Surface phosphate	mmol-P m^{-3}
Bottom Stress	N m^{-2}	Surface Chl *a*	mg m^{-3}
Surface temperature	°C	Primary production (0-40 m North Sea, 0-20 m IDW)	mg-C m^{-2} d^{-1}
Surface salinity	psu	Surface zooplankton biomass	mmol-N m^{-3}
Light attenuation (Kd)	m^{-1}	Zooplankton production (0-40 m NS, 0-20 m IDW)	mg-C m^{-2} d^{-1}
		Bottom oxygen	mg l^{-1}
		Benthos biomass	mmol-N m^{-3}

4.2 Sensitivity analysis

The ecosystem variable responses (*VR*, %) were estimated as the difference between each scenario (*SCE*) and the REF-NO-FARM scenario (*REF*) divided by the mean of *REF* and multiplied by 100% for each grid cell (Daewel et al. 2022):

$$VR_i = \frac{\int_{i=1}^{n}(SCE_i - REF_i)}{mean(REF)} \times 100\% \qquad \text{(eq. 6)}$$

The *VR* was estimated for each day=*i* during the summer productive period from April to October (*n*=211 days). Changes in spring bloom dynamics were not included in this estimate, since we focused on the summer production with the strongest seasonal stratification (Figure 3.1). However, changes in PEA and primary production were analyzed for seasonal patterns.

The *VR* did not follow a normal distribution and were better summarized by using medians and percentiles rather than means and standard deviations. Means can be highly affected by outliers, even though they impact only a small fraction of the response, whereas percentiles are based on the ordering of the data (Figure 4.1). The 50th

percentile is equal to the median, where half of the daily values are above, and half are below. If the values are distributed around zero, the median will be close to zero due to the cancellation of negative/positive values. Instead, upper and lower percentiles can be used to access the distribution range in the spatial mapping of responses. The 5th and 95th percentiles represent the bottom 5% and top 5% of the data, respectively. Hence, the percentile range (between the 5th and 95th percentiles) represents the changes for 90% of the days (190 days).

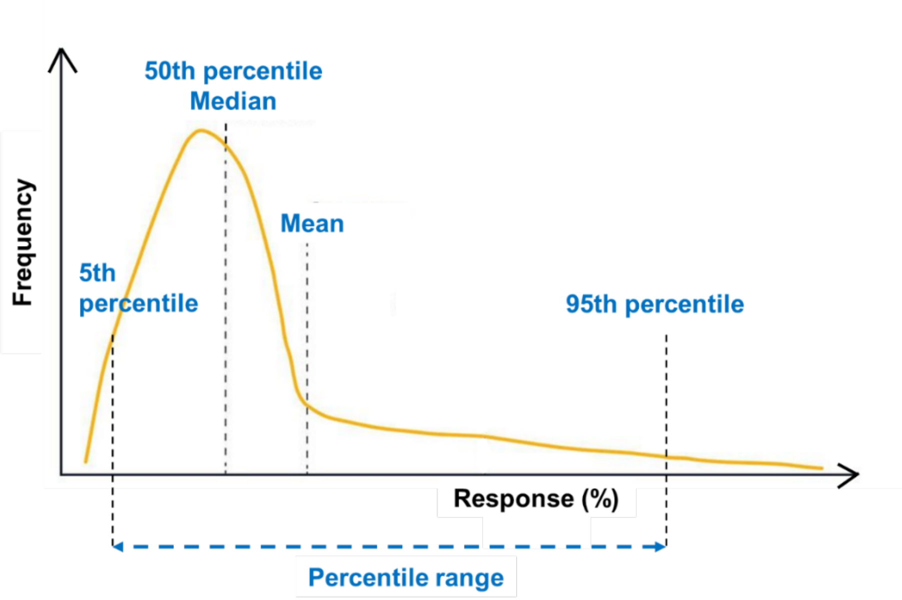

Figure 4.1. Percentiles are used to assess the variable responses to offshore wind. The median (50th percentile) means that 50% of the responses will be above and 50% below. The "mean" is the weighted mean. For the 95th percentile, 95% of the data is below and 5% above. The percentile range is the interval between the 5th and 95th percentiles. Example from a long-tail distribution for illustration, not to scale.

The spatial impact index (*S*-index) was estimated for PEA and primary production for the two scenarios (*SCE*), CURRENT and Y2030. The absolute median of the difference between *SCE* and REF-NO-FARM (*REF*) was divided with the standard deviation (STD) of *REF* for each model grid cell over time:

$$S - \text{index} = \frac{|Median(SCE - REF)|}{STD_{REF}} \times 100\% \qquad \text{(eq. 7)}$$

The *S*-index estimates the change in the scenarios relative to the daily natural variability of the system (expressed as the standard deviation). A higher value indicates a higher impact, where e.g. a *S*-index=10% means that the found median change is equal to 10% of the natural variability. Values below 0.1% were removed from the plots for better visualization. The *S*-index was estimated for the entire model domains of the North Sea and the Inner Danish waters as well as for the Danish Exclusive Economic Zone (EEZ) in both study areas.

It is important to note that the sensitivity analysis is based on scenarios with all the offshore wind farms included at the same time. It was not possible to run each wind farm individually due to time restrictions.

5 Sensitivity to offshore wind in the North Sea

5.1 Ecosystem responses in the North Sea

Spatial responses of the 14 selected ecosystem variables (*VR*) in the Y2030 scenario relative to REF-NO-FARM from April to October were calculated as: a) 5th percentile, b) median (50th percentile) and c) 95th percentile. Hence, the percentile range is the found interval of responses, where a high range indicates high variability around the median. The results of physical variables are shown in Figures 5.1-5.6 and for biogeochemical variables in Figures 5.7-5.14. The offshore wind farms are indicated as red points, and the scale varies between plots (color bars). The spatial ranges of medians and percentiles are summarized for the entire model domain in Table 5.1 and for the Danish EEZ in Table 5.2. The absolute percentile range is the absolute distance between the 5th and 95th percentile rounded to nearest integer.

Table 5.1. Summary of model results for the spatial plots shown in the figures 5.1.1-14 for each ecosystem variable in the North Sea (whole model domain) in Y2030 from April to October.

	Y2030			
North Sea model domain	**Medians (%) median / min / max**	**Absolute median range (%)**	**Percentiles (%) min / max**	**Absolute percentile range (%)**
Physical variables:				
Stratification index (PEA)	0.000 / -30.2 / 8.3	39	-86.4 / 32.2	119
Surface current speed	-0.044 /-0.4 / 0.2	1	-5.3 / 1.7	7
Bottom stress	-0.034 / -0.8 / 0.7	2	-4.5 / 3.9	8
Surface temperature	0.142 / -2.2 / 0.8	3	-7.2 / 3.2	10
Surface salinity	0.000 /-0.4 / 0.1	1	-0.5 / 0.1	1
Light attenuation Kd	0.013 / -0.2 / 5.0	5	-4.0 / 8.2	12
Biogeochemical variables:				
Surface nitrate	0.069 / -3.0 / 13.3	16	-5.1 / 34.8	40
Surface phosphate	-0.001 / -1.0 / 38.5	40	-5.8 / 90.4	96
Surface Chl *a*	-0.061 / -7.5 / 6.1	14	-17.1 / 10.3	27
Primary production (0-20 m)	0.014 /-2.4 / 43.7	46	-6.5 / 81.1	88
Surface zooplankton biomass	-0.064 / -9.6 / 1.8	11	-16.2 / 6.9	23
Zooplankton production (0-20 m)	0.089 / -0.8 / 5.7	7	-4.9 / 12.7	18
Bottom oxygen	0.009 / -0.2 / 1.4	2	-0.8 / 2.0	3
Benthos biomass	0.009 / -1.5 / 0.5	2	-5.1 / 1.2	6

Physical variables in the North Sea:

The physical variables that showed the highest variability in the response to offshore wind farm development were stratification index (PEA) followed by Kd and surface temperature in the North Sea, as seen from the percentile range (Table 5.1). Median responses were highest for PEA (-30.2% to 8.3%), surface temperature (-2.2% to 0.8%) and Kd (-0.2% to 5.0%). On average for the North Sea, surface temperatures showed the highest change with +0.142%.

The PEA median values showed a decrease inside and close to the offshore wind farm areas and the opposite response in the neighboring area (Figure 5.1). The UK farms had a higher wind capacity per area and in areas with stronger currents (Figure A1.3b). Those farms therefore caused a stronger decrease in PEA due to monopile mixing compared to the other countries. Generally, higher current speeds caused higher mixing and a decrease in PEA compared to wind farms located in more stratified waters with lower current speeds (see section 5.3). For instance, the German wind farms located far from land showed lower changes because current speeds were lower (<0.15 m s^{-1}) and the wind wake effect cancelled out the monopile drag effect

For all physical variables, except for salinity, there was a high temporal variability in the responses seen from the 5th and 95th percentiles, which showed both negative and positive changes, respectively. Hence, the median values were often close to zero, although the daily values showed higher variability (Table 5.1). Current speeds and bottom stress mainly decreased in the southeastern parts (Figure 5.2-3). Surface temperature increased in areas with increased stratification due to solar heating. In areas with reduced stratification, temperature decreased due to mixing with cooler bottom water (Figure 5.4). Salinity showed small change (Figure 5.5). Light attenuation increased in the areas within or close to the offshore wind farms and decreased further away (Figure 5.6).

In the Danish EEZ, the physical variables showed less strong responses than for the North Sea model domain (Table 5.2). Median responses were highest for PEA (-8.1% to 1.3%), but on average showed no change for the EEZ. On average, current speed showed a decrease of -0.127%, and surface temperature showed an increase of 0.126%.

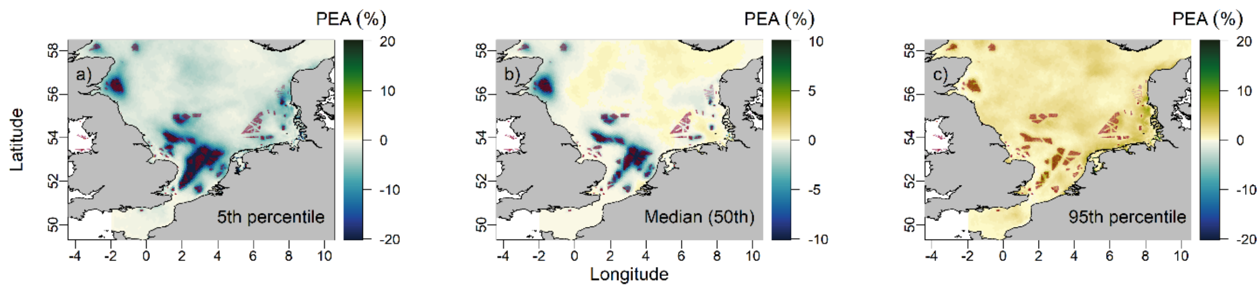

Figure 5.1. Response in PEA (0-40 m) for the Y2030 scenario.

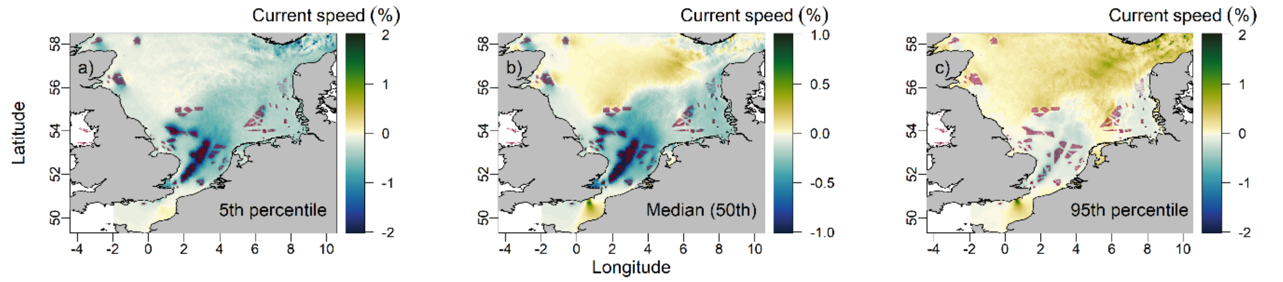

Figure 5.2. Response in surface current speed for the Y2030 scenario.

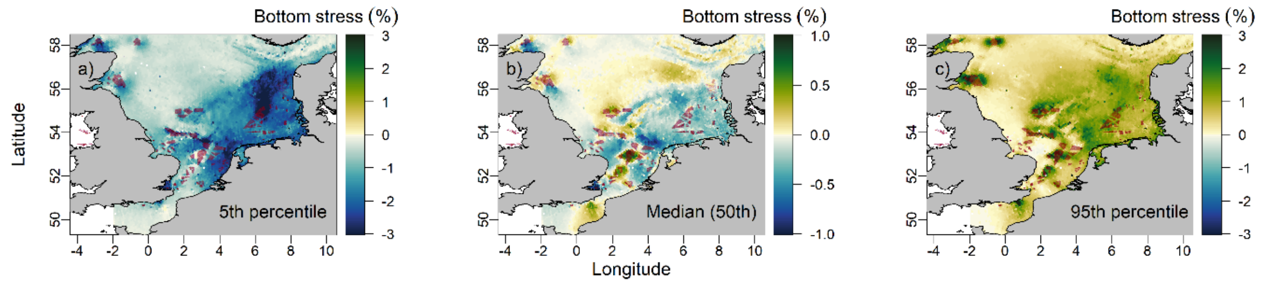

Figure 5.3. Response in bottom stress for the Y2030 scenario.

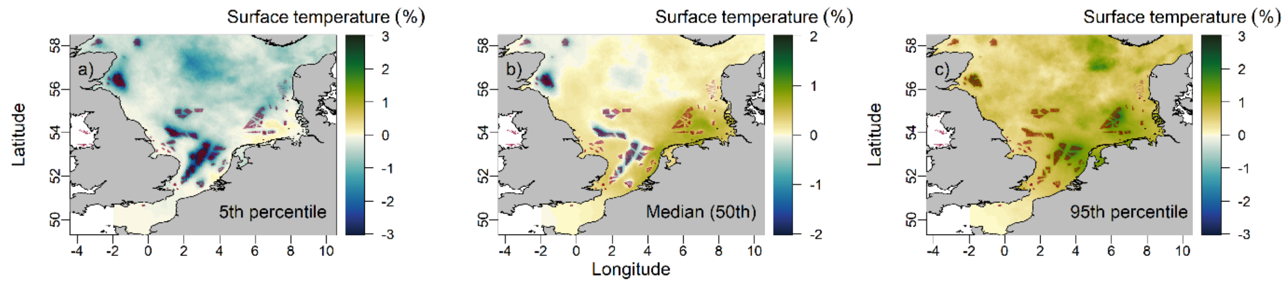

Figure 5.4. Response in surface temperature for the Y2030 scenario.

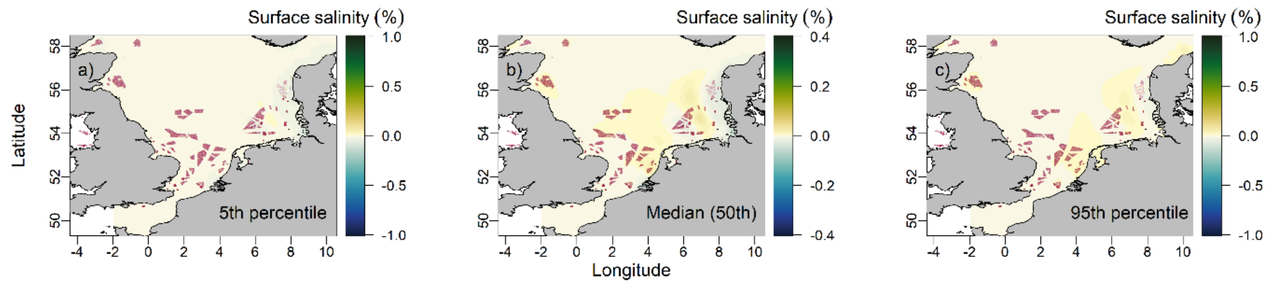

Figure 5.5. Response in surface salinity for the Y2030 scenario.

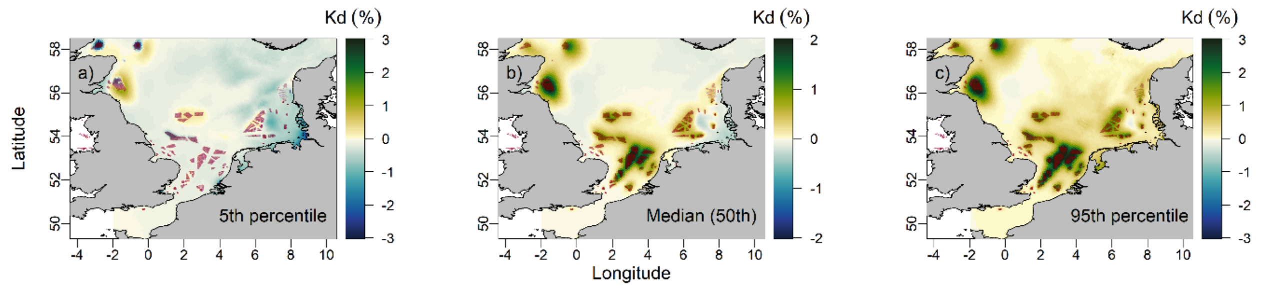

Figure 5.6. Response in light attenuation (Kd) for the Y2030 scenario.

Biogeochemical variables in the North Sea:

The biogeochemical variables with the highest percentile range (variability) of responses to offshore wind farm development in the North Sea were primary production and phosphate concentrations (Table 5.1). Median responses were highest for primary production (-2.4% to 43.7%) and phosphate concentration (-1.0% to 38.5%). On average for the North Sea, the highest response was for zooplankton production (+0.089%).

Median responses of nitrate and phosphate decreased in the central part of the North Sea, but increased inside offshore wind farm areas (Figures 5.7, 5.8). Median responses of Chl *a* concentrations increased in the offshore wind farms, except in the English Channel (Figure 5.9). Zooplankton biomass both decreased and increased in different wind farm areas (Figure 5.11). Median responses of primary- and zooplankton production increased by a maximum of 43.7% and 5.7%, respectively, in the offshore wind farms (Figure 5.10, 5.12). Bottom oxygen increased slightly (<1.4%) in most areas due to more mixing (Figure 5.13). Benthos biomass decreased in the areas with more mixing and increased elsewhere, overall with <1.5% median change (Figure 5.14).

In the Danish EEZ, the variable responses were lower than for the entire North Sea (Table 5.2). Median responses were highest for nitrate concentration (-1.2% to 0.7%), phosphate concentration (-0.7% to 4.7%), primary production (-0.5% to 1.6%) and zooplankton production (-0.5% to 1.0%). On average, zooplankton production increased the most with 0.176%.

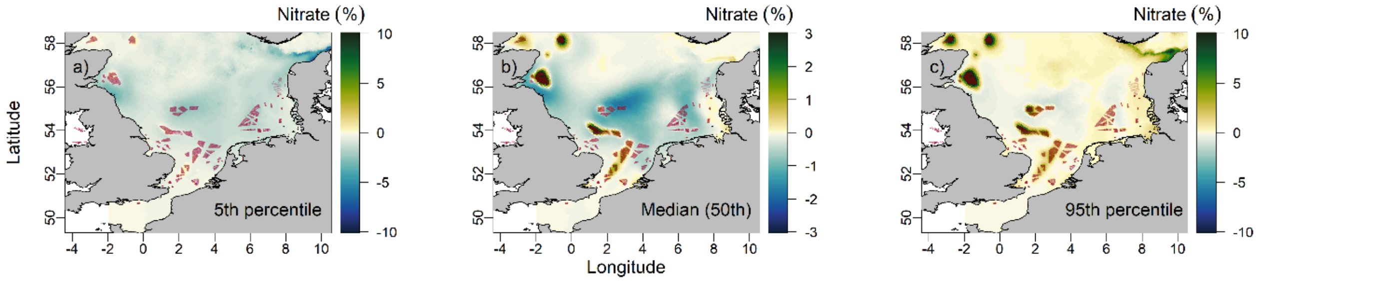

Figure 5.7. Response in surface nitrate for the Y2030 scenario.

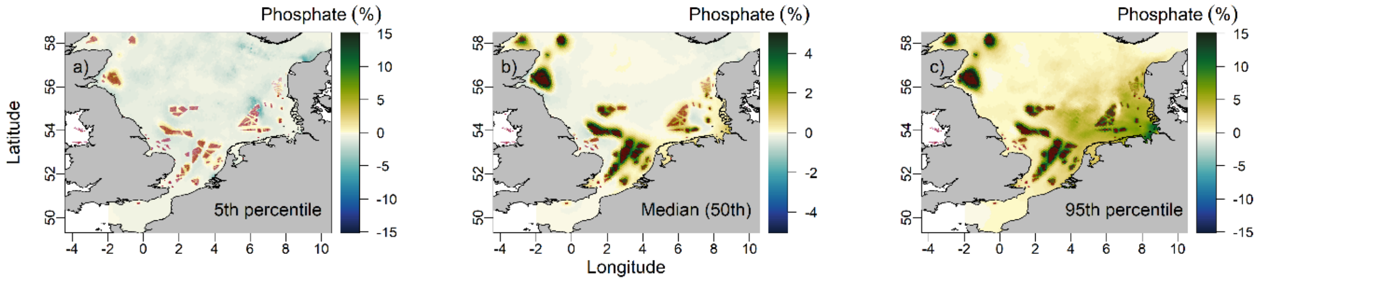

Figure 5.8. Response in surface phosphate for the Y2030 scenario.

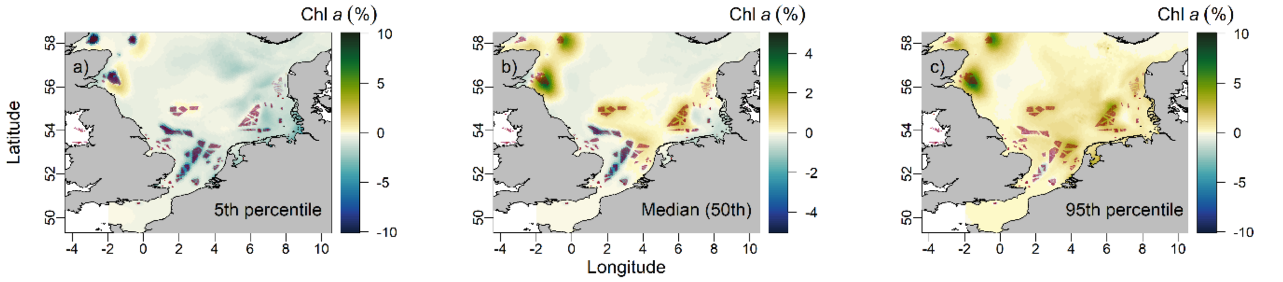

Figure 5.9. Response in surface Chl *a* concentration for the Y2030 scenario.

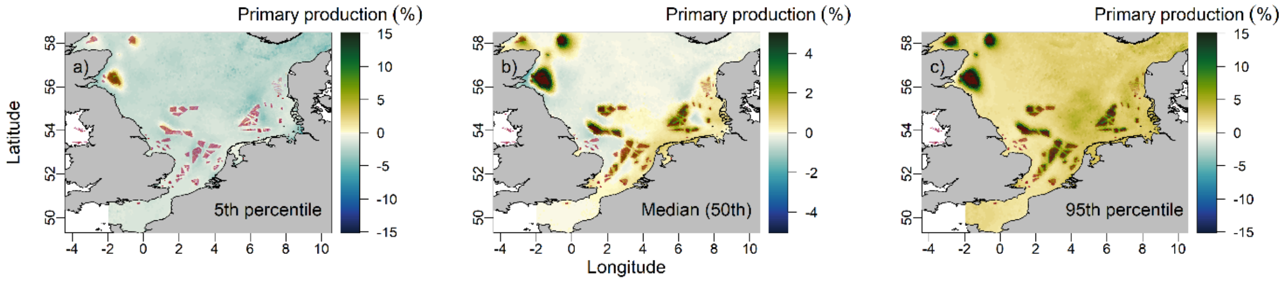

Figure 5.10. Response in depth-integrated primary production (0-40 m) for the Y2030 scenario.

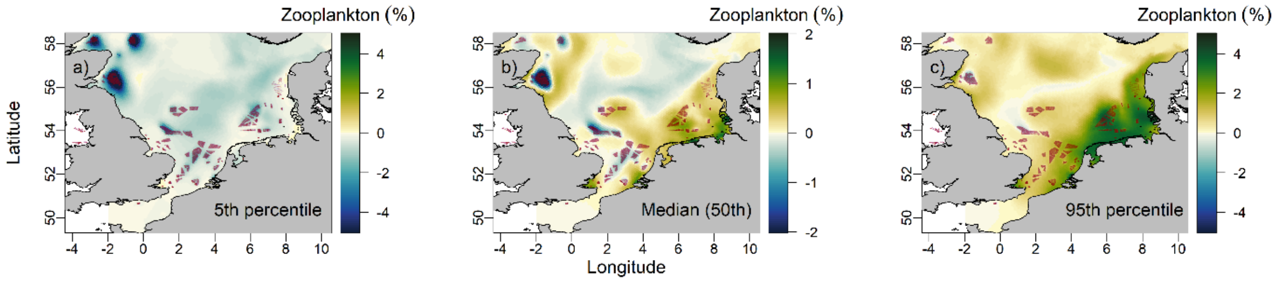

Figure 5.11. Response in surface zooplankton biomass for the Y2030 scenario.

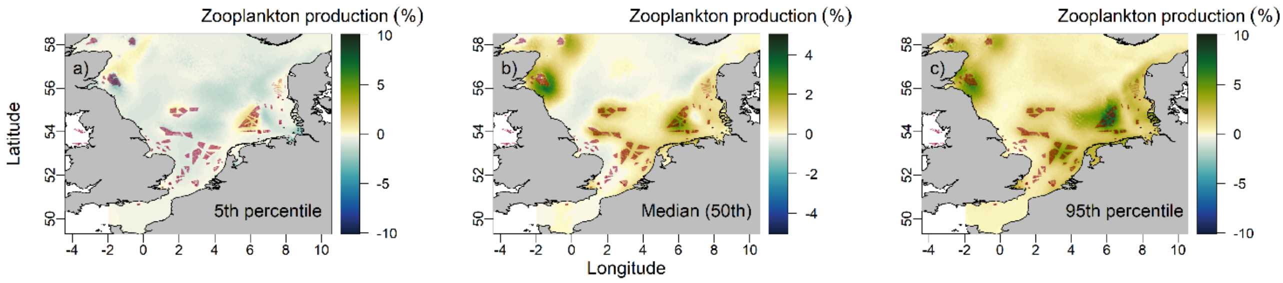

Figure 5.12. Response in zooplankton production (0-40 m) for the Y2030 scenario.

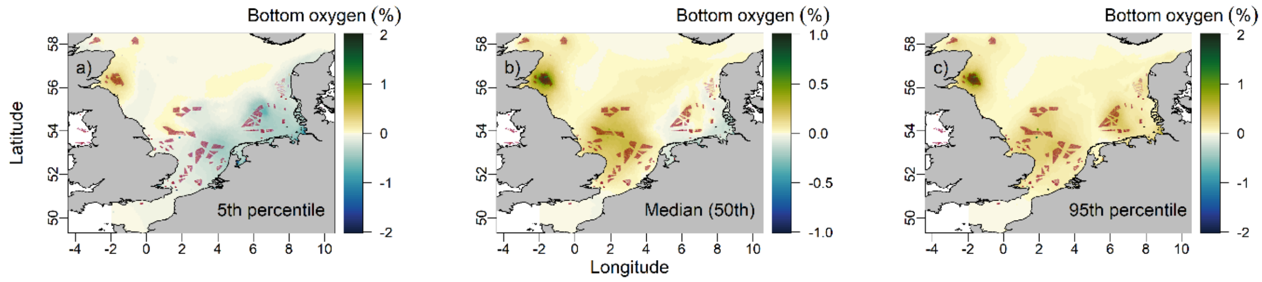

Figure 5.13. Response in bottom oxygen for the Y2030 scenario.

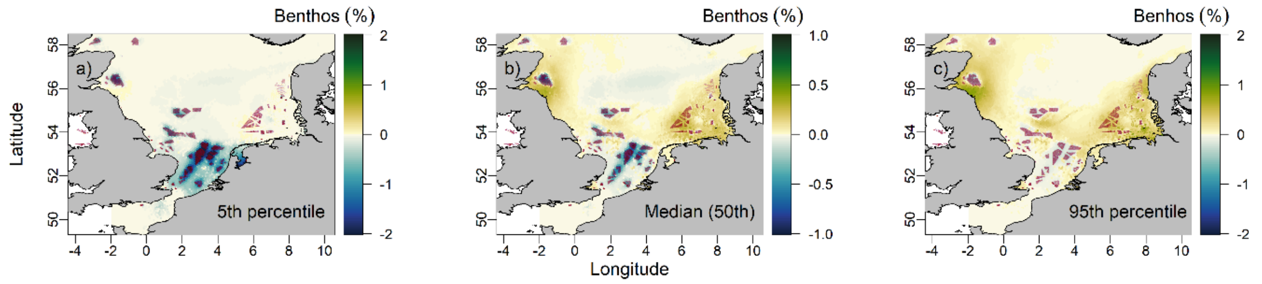

Figure 5.14. Response in benthos biomass for the Y2030 scenario.

Table 5.2. Summary of model results for the spatial plots shown in the figures 5.1.1-14 for each ecosystem variable in the North Sea Danish EEZ in Y2030 from April to October.

	Y2030			
North Sea DK EEZ	**Medians (%) median / min / max**	**Absolute median range (%)**	**Percentiles (%) min / max**	**Absolute percentile range (%)**
Physical variables:				
Stratification index (PEA)	0.000 / -8.1 / 1.3	9	-17.1 / 18.5	36
Surface current speed	-0.127 /-0.9 / 0.2	1	-2.6 / 1.7	4
Bottom stress	-0.079 / -0.4 / 0.3	1	-3.6 / 2.9	7
Surface temperature	0.126 / -0.3 / 0.4	1	-1.1 / 1.2	2
Surface salinity	-0.004 /0.0 / 0.0	0	-0.1 / 0.1	0
Light attenuation Kd	-0.040 / -0.3 / 1.0	1	-0.9 / 1.7	3
Biogeochemical variables:				
Surface nitrate	0.200 / -1.2 / 0.7	2	-7.3 / 10.3	18
Surface phosphate	-0.047 / -0.7 / 4.7	5	-5.8 / 9.0	15
Surface Chl *a*	-0.062 / -0.5 / 0.5	1	-2.2 / 2.2	4
Primary production (0-20 m)	-0.031 /-0.5 / 1.6	2	-5.1 / 7.3	12
Surface zooplankton biomass	0.127 / -0.4 / 0.5	1	-1.3 / 3.3	5
Zooplankton production (0-20 m)	0.176 / -0.5 / 1.0	2	-1.5 / 4.1	6
Bottom oxygen	0.013 / -0.1 / 0.1	0	-0.8 / 0.6	1
Benthos biomass	0.015 / -0.2 / 0.2	0	-0.8 / 0.7	2

5.2 Responses of PEA and primary production inside the offshore wind farms for Y2030

PEA and primary production showed some of the strongest responses to offshore wind farm development (Table 5.1) and are therefore analyzed in more detail inside the offshore wind farm areas. The wind farm areas were defined as the model polygons with at least one wind turbine. The seasonal response of PEA in Y2030 relative to REF-NO-FARM showed slightly higher stratification in winter and more mixing during summer when the water column was more stratified (Figure 3.1, Figure 5.15a). For the entire North Sea, responses were ten times lower compared to the offshore wind farm areas (Figure 5.15c). Primary production showed the highest change in March during the phytoplankton spring bloom and later in September (Figure 5.15b). The seasonal pattern of primary production mainly showed positive responses in the offshore wind farms, although the spring bloom was delayed (negative values beginning of March). In the entire North Sea, responses in primary production were lower and with no clear direction (Figure 5.15d).

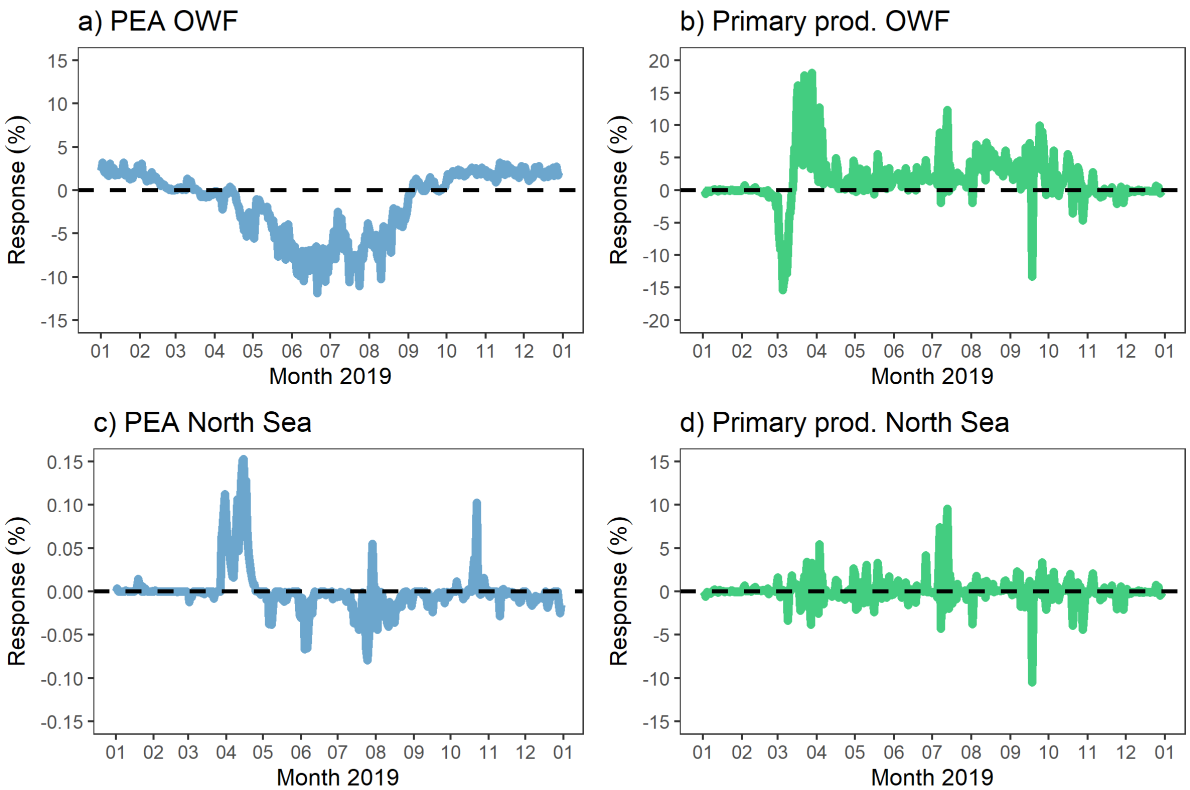

Figure 5.15. Time-series responses (%) of a) stratification index (PEA) and b) primary production estimated as median values only inside the offshore wind farm areas and c) stratification index (PEA) and d) primary production in the whole North Sea in Y2030. Note the different scales.

The responses of PEA and primary production were analyzed against changes in wind speed (wind wake effect on x-axis) and mean current speed (color scale) in the offshore wind farm areas (Figure 5.16). A decrease in wind speed was expected to give a stronger stratification and reduce primary production (less vertical mixing of nutrients). A faster mean current speed was expected to result in a stronger monopile drag causing, less stratification and more mixing of nutrients to the surface layer, thereby increasing primary production.

In Y2030, PEA was found to generally decrease with less wind speed (stronger wind wake) in contrast to our expectations (Figure 5.16a). Only for weak current speeds, PEA increased with less wind speed (yellow-orange color in Figure 5.16a). For increasing current speeds, stratification decreased due to more monopile mixing as expected. Hence, this showed that for the offshore wind farm areas in the North Sea, monopile mixing had a stronger effect on PEA than the wind wakes at high current speeds (>0.15 m s^{-1}). This result agreed with a previous model study showing that monopile-induced mixing was significantly stronger than the wind wake effect in the German Bight due to strong tidal currents (Christiansen et al. 2023).

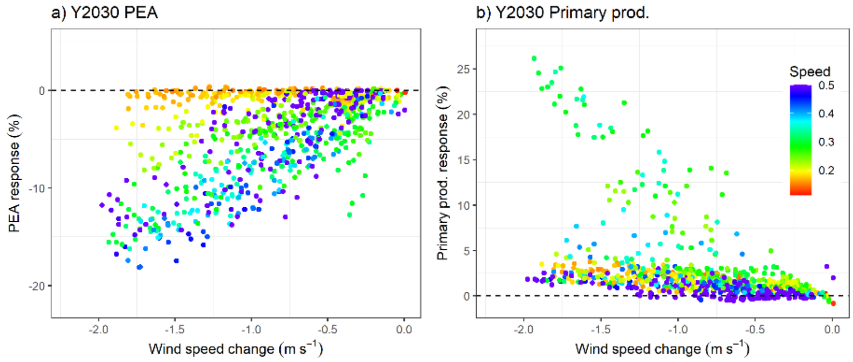

Figure 5.16. Median responses (%) for each model polygon with offshore wind farms of a) PEA and b) primary production in Y2030 to changes in wind speed (x-axis) and mean current speed (color scale) in REF-NO-FARM. C) Mean PEA in REF-NO-FARM versus changes in wind speed in the corresponding Y2030 scenario. Blue colors are high current speeds and yellow-orange colors are low current speeds.

Primary production inside the offshore wind farm areas did not decrease with decreasing wind speeds as expected. Instead, the monopile mixing effect seemed to be stronger than the wind wake effect, causing increased mixing of nutrients to the surface layer stimulating primary production (Figure 5.16b). However, the response to mean current speed seemed to be dome shaped. At high (blue color) and low (yellow-orange colors) current speeds, primary production increased less than for intermediate (green colors) current speeds.

At high current speeds, the water column is almost fully mixed (PEA<10 J m^{-3}, Figure 5.16c) and primary production will not be affected by increased vertical transport of nutrients. At low current speeds, the monopile drag effect on mixing is weaker and, hence, also affects stratification and primary production less. At intermediate current speeds (0.25-0.40 m s^{-1}) in stratified waters (Figure 5.16c), the higher mixing from the monopiles caused vertical transport of nutrients from the bottom to the surface layer, stimulating primary production. However, at these intermediate current speeds there is also the highest areal density of offshore wind farms that may cause cumulative effects between the different wind farms (Figure 3.2). A previous model study from the North Sea likewise found that different hydrodynamic regimes affected the responses of primary production to offshore wind showing a primarily increase in the German Bight and central southern parts (van Duren et al. 2021).

5.3 Spatial impact index for the North Sea and the Danish EEZ

PEA in the North Sea area:

The spatial impact index is the median change relative to the natural variability. For PEA, the spatial impact index in CURRENT showed the highest effect near the wind farm areas in the North Sea area (Figure 5.17a). For Y2030, the spatial impact index was higher (maximum 34%) than for CURRENT, extending further outside the offshore wind farm areas (Figure 5.17c). The outermost planned offshore wind farm in the German Bight showed low impact on PEA because it was placed in stratified waters with low current speed causing less monopile mixing that was counteracted by the wind wake effect. The wake effect caused more diffuse responses over a larger area than the local monopile mixing. Overall, neighboring wind farms affected each other and caused cumulative effects in a wider area of the North Sea.

PEA in the Danish EEZ:

In the DK-EEZ, the impact was highest inside the offshore wind farm areas with maximum 20% of the natural variability, but relatively low outside in both scenarios (Figure 5.17b, d). In the largest planned Danish offshore wind farm areas in Y2030 (Thor and Nordsøen I), the impact was lower (<3%) than for the existing wind farms (Figure 5.17d). This was probably due to a lower number of wind turbines per model grid cell (Figure 1.2b) and therefore lower monopile mixing effects (Figure 1.3a). Generally, the impact of the Danish offshore wind farms was less than for the other countries, probably due to a lower number of wind turbines per model grid cell. The impact range was approximately less than 5 km from the wind farms in the North Sea.

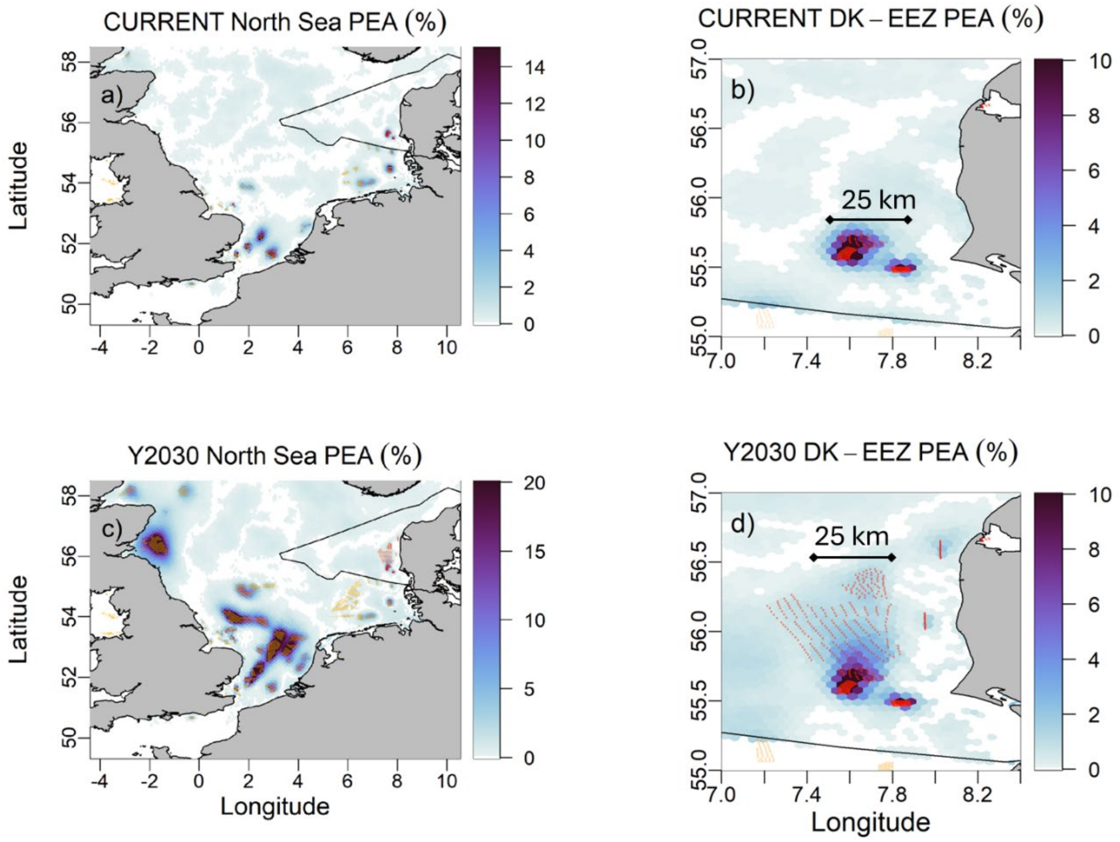

Figure 5.17. PEA spatial impact index (%) in a) CURRENT the North Sea (max. value = 23%), b) CURRENT the DK-EEZ (max. value=20%), c) Y2030 the North Sea (max. value = 34%), and d) Y2030 the DK-EEZ (max. value= 20%). Offshore wind farms are indicated as red points in the Danish EEZ and orange points outside Denmark and the DK-EEZ is shown as a black solid line. The DK-EEZ is influenced by offshore wind farms in both Denmark and other countries. Values below 0.1% were omitted in the plots.

Primary production in the whole North Sea:

For primary production, the spatial impact index in CURRENT (max. 12%) showed the highest effect inside and close to the wind farm areas in the North Sea (Figure 5.18a). For Y2030, the spatial impact index was higher (max. 144% in Scotland) than in CURRENT and the impact extended outside the offshore wind farm areas (Figure 5.18c). However, the assumed offshore wind farms off the coast of Scotland are extensive and of very high installed capacity density (~12 MW km^{-2}) that might have be overestimated in the Y2030 scenario (Hahmann et al. 2025). Overall, neighboring wind farms caused cumulative effects in a wider area as seen for PEA.

Primary production in the Danish EEZ:

In the DK-EEZ, the maximum impact was 5% of the natural variability in both CURRENT and Y2030 (Figure 5.18b, d). The impact was highest inside the offshore wind farm areas for both scenarios, but the Y2030 showed higher effects outside the wind farm areas compared to CURRENT. As for PEA, the planned Danish offshore wind farms showed a lower impact than the established ones and for other countries. It was difficult to estimate an impact range, since the neighboring wind farms affected each other and the pattern was rather smooth. Still, less than 5 km away from the wind farms, the impact was very small.

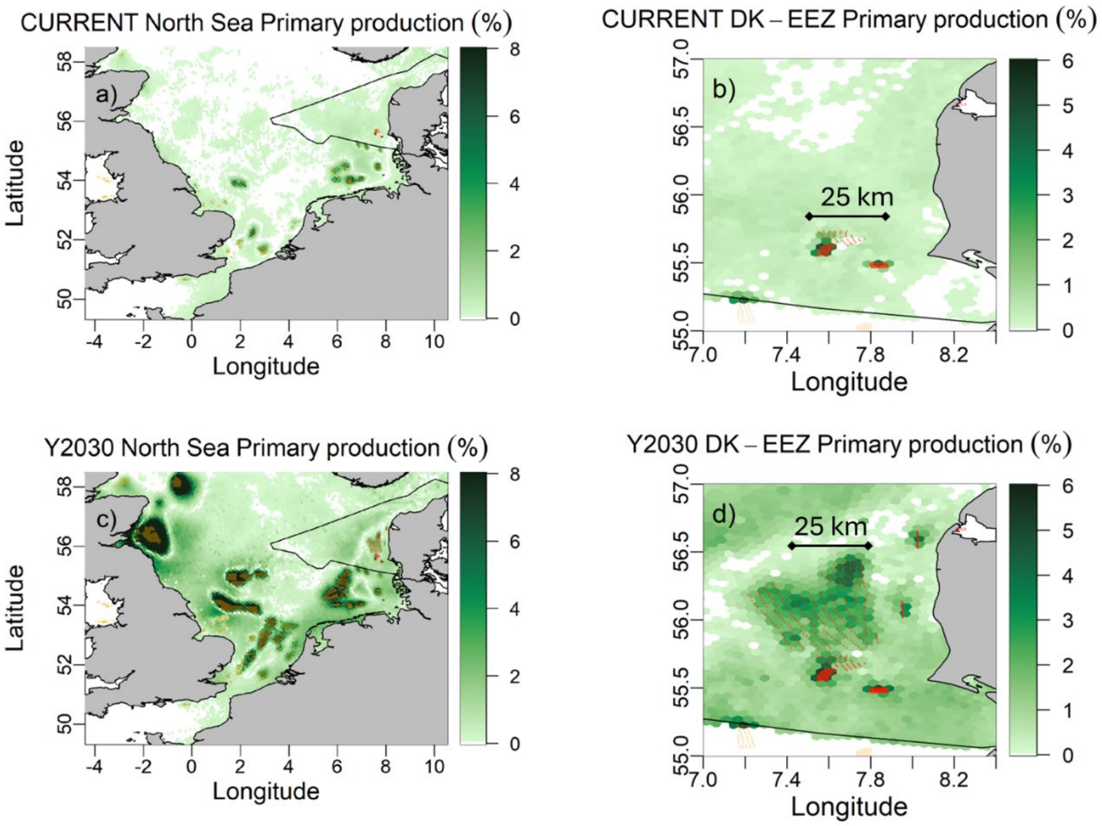

Figure 5.18. Primary production spatial impact index (%) in a) CURRENT the North Sea (max. value = 12%), b) CURRENT the DK-EEZ (max. value=5%), c) Y2030 the North Sea (max. value = 144%), and d) Y2030 the DK-EEZ (max. value= 5%). Offshore wind farms are indicated as red points in the Danish EEZ and orange points outside Denmark and the DK-EEZ is shown as a black solid line. The DK-EEZ is influenced by offshore wind farms in both Denmark and other countries. Values below 0.1% were omitted in the plots.

5.4 Extreme events

Modelled and spatially averaged PEA differences in the Danish sector of the North Sea (blue rectangle in Figure 5.19a) between the Y2030 scenario and REF-NO-FARMS were generally small throughout the year and between extreme wind conditions (Figure 5.19c, d). Under stronger wind conditions, a moderate stabilization of the stratification was predicted in the simulations (Figure 5.19d). The North Sea is generally well-mixed in many regions, with PEA changes predominantly influenced by tidal and wind mixing. The wake effect from offshore wind farms became slightly more pronounced during periods of stable atmospheric conditions and wind speeds around highest turbine thrust coefficients, leading to a slight enhancement in PEA. However, the differences in PEA were minimal, amounting to ≤ 0.5% of the total PEA in the selected area. The situation in the eastern North Sea sometimes strongly contrasts with conditions in other areas proposed for wind farm extension in the southern and western parts of the North Sea. In these latter areas, stratification is typically more pronounced for the reference scenario (Figure 5.19a, b). This highlights a distinct regional variation in how wind conditions affect stratification, suggesting that localized factors, such as background currents and tidal mixing, may play a significant role in the overall PEA response across different parts of the North Sea. However, the monopile density is also important for the impact and this was relatively low in the Danish sector.

Figure 5.19. Modelled differences of PEA (J m^{-3}) the North Sea model between the 2030 scenario and REF-NO-FARM. (a, b) Spatial maps showing PEA during CALM and WINDY periods. (c) Time series of PEA averaged inside the Danish sector of the North Sea (blue rectangle in (a) and (b). (d) Box plots of modelled changes in PEA during different wind conditions. Black horizontal bars represent the median. Colored boxes show the 25% and 75% quartiles. Whiskers extend two times the interquartile range indicating the range of values between minimum and maximum across the interquartile. The analysis is based on 3-hourly model output. CALM and WINDY periods are indicated in Table 1.2.

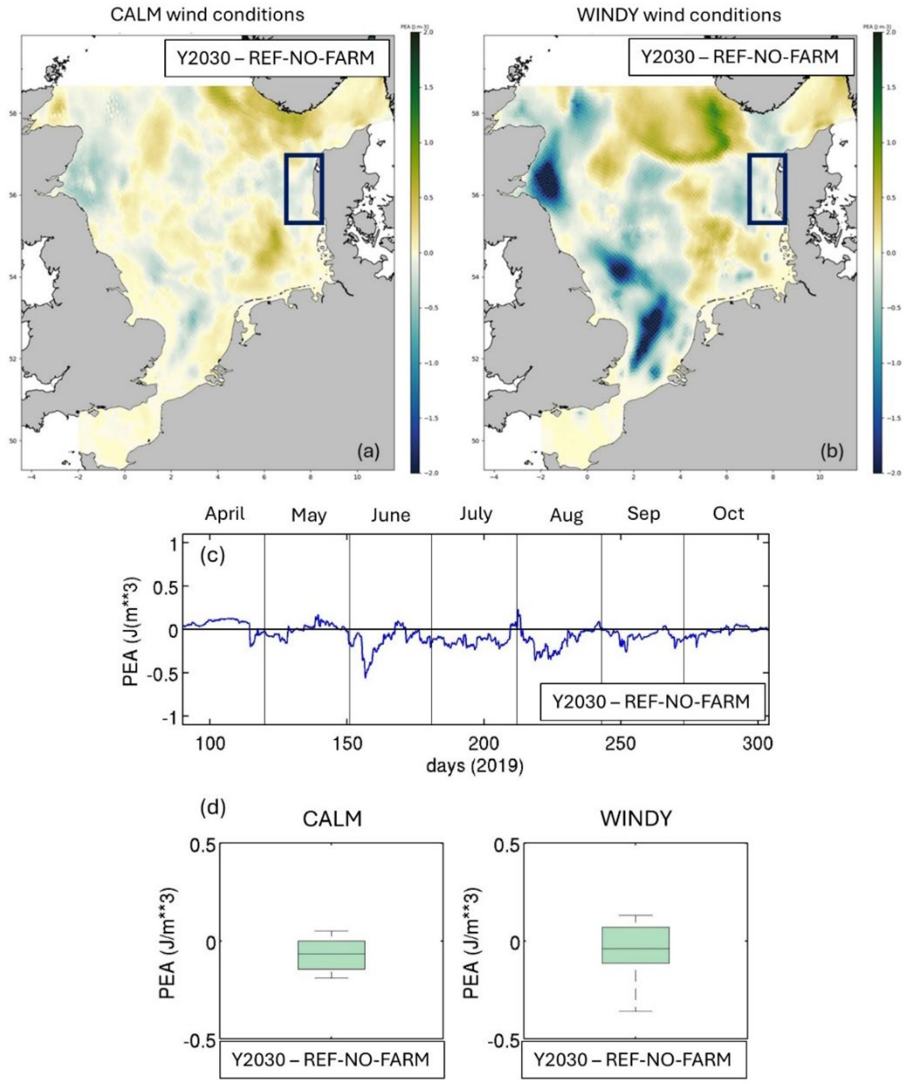

6 Sensitivity to offshore wind in the Inner Danish waters

6.1 Ecosystem responses of the Inner Danish waters

Spatial responses of the 14 selected ecosystem variables in the Y2030 scenario relative to REF-NO-FARM from April to October for the Inner Danish waters are shown as: a) 5th percentile, b) median (50th percentile), and c) 95th percentile of physical variables (Figures 6.1-6) and biogeochemical variables (Figures 6.7-14). The offshore wind farms are indicated as red points and the scale on the color bar varies between plots. The spatial ranges of medians and percentiles are summarized for the entire model domain in Table 6.1 and for the Danish EEZ in Table 6.2. The absolute median range is the distance between the lowest and highest median values rounded to nearest integer. The absolute percentile range is the distance between the 5th and 95th percentiles rounded to the nearest integer. There was a high temporal variability in the responses, as seen from the 5th and 95th percentiles, which showed both negative and positive changes, respectively. Hence, the median values were often close to zero, although the daily values showed higher variability.

In the southeastern part of the study area (outside the Oder Lagoon), the wind speed showed an increase in both scenarios due to atmospheric compensating mechanisms (Figure 1.3b, d). The increased wind speeds caused an upwelling of bottom water to the surface, and the model showed strong effects of physical and biogeochemical variables compared to the larger area. Future sensitivity studies of both the atmospheric and marine models are needed to evaluate if the found changes are caused by some kind of bias in the models or if this effect could be realized.

Physical variables in the Inner Danish waters:

In the Inner Danish waters model domain, the ecosystem variables that showed the highest variability in the responses to offshore wind farm development were PEA, Kd, surface temperature and bottom stress in both scenarios according to the percentile range (Table 6.1). Median responses were highest for PEA (-2.5% to 3.1%) and surface temperature (-0.7% to 2.6%) in Y2030. On median average, the highest response was found for surface temperature (0.026%).

PEA generally increased in a larger area around the offshore wind farms and decreased in neighboring areas without wind farms (Figure 6.1, Table 6.1). Current speed and bottom stress decreased in most of the Inner Danish waters due to the wake effect from offshore wind farms, except for a few spots (Figures 6.2, 6.3). Surface temperature increased in the areas with stronger stratification due to less mixing with the cooler bottom water (Figure 6.4). Surface salinity showed low responses (Figure 6.5). Surface Kd increased in most areas due to higher surface Chl *a* concentration (Figures 6.6, 6.9). Another model study also found that offshore wind farms would increase summer sea surface temperatures and rise the halocline depth (indicator of stratification) in the Arkona Basin (Arneborg et al. 2024).

In the Danish EEZ, the median values and percentile ranges of the physical variables were in most cases similar to the Inner Danish waters model domain, except for Kd influenced by the Oder Lagoon (Table 6.2). Median responses were highest for PEA (-3.3% to 4.1%) and surface temperature (-0.3% to 1.0%) in Y2030. On median average, the highest response was found for surface temperature (0.072%).

Table 6.1. Summary of model results for the spatial plots shown in the figures 6.1.1-14 for each ecosystem variable in the Inner Danish Waters (whole model domain) in Y2030 from April to October.

	Y2030			
Inner Danish waters model domain	**Medians (%) median / min / max**	**Absolute median range (%)**	**Percentiles (%) min / max**	**Absolute percentile range (%)**
Physical variables:				
Stratification index (PEA)	0.004 / -2.5 / 3.1	6	-13.9 / 19.5	33
Surface current speed	-0.003 /-0.4 / 0.2	1	-1.6 / 1.4	3
Bottom stress	-0.004 / -0.8 / 0.2	1	-5.2 / 8.0	13
Surface temperature	0.026 / -0.7 / 2.6	3	-3.4 / 7.6	11
Surface salinity	0.002 /-0.4 / 0.1	1	-0.9 / 0.6	2
Light attenuation Kd	0.010 / -0.3 / 0.5	1	-2.1 / 18.2	20
Biogeochemical variables:				
Surface nitrate	0.007 / -1.8 / 2.7	5	-37.0 / 46.9	84
Surface phosphate	0.005 / -1.1 / 4.3	5	-13.5 / 16.7	30
Surface Chl *a*	0.043 / -0.8 / 2.9	4	-6.9 / 42.3	49
Primary production (0-20 m)	-0.008 /-5.2 / 1.7	7	-39.3 / 43.2	83
Surface zooplankton biomass	-0.036 / -1.7 / 2.4	4	-10.6 / 19.8	30
Zooplankton production (0-20 m)	-0.016 / -8.1 / 2.9	11	-19.2 / 20.5	40
Bottom oxygen	0.004 / -1.4 / 0.6	2	-2.9 / 2.2	5
Benthos biomass	-0.002 / -0.1 / 0.0	0	-0.8 / 0.4	1

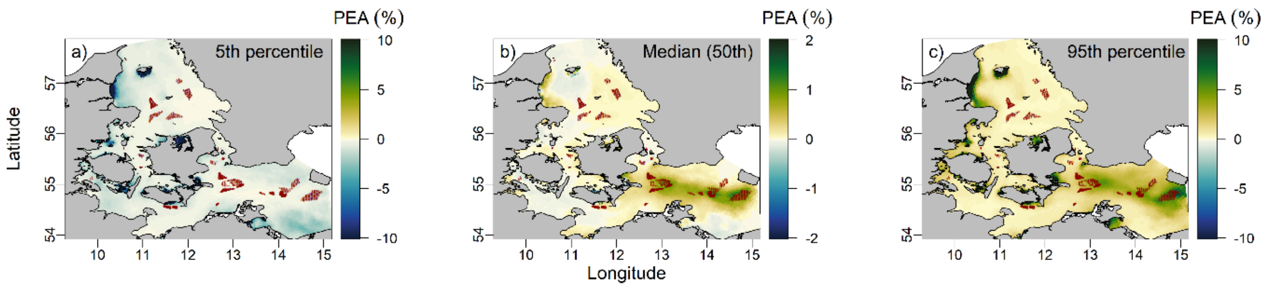

Figure 6.1. Changes in stratification index (0-20 m) for the Y2030 scenario.

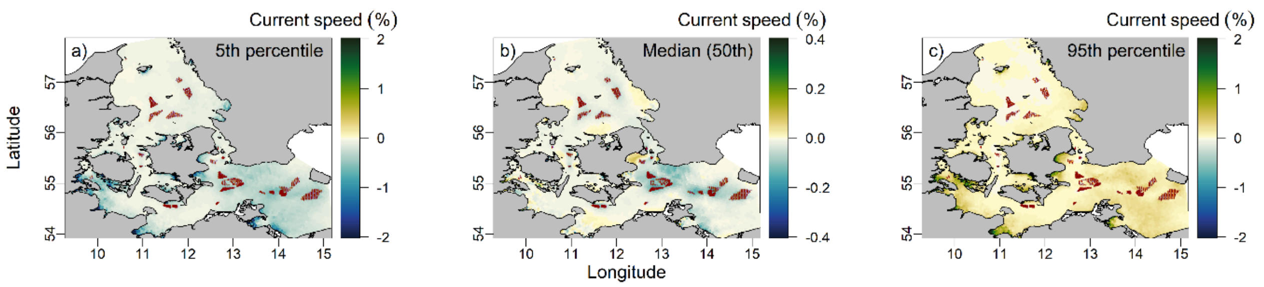

Figure 6.2. Changes in surface current speed for the Y2030 scenario.

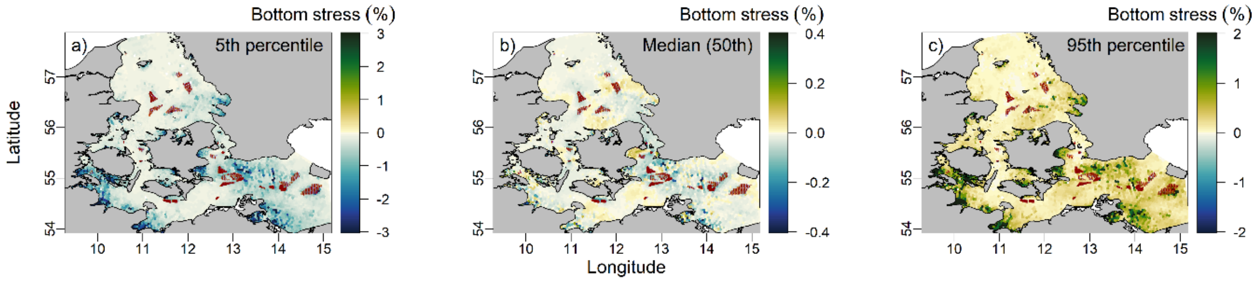

Figure 6.3. Changes in bottom stress for the Y2030 scenario.

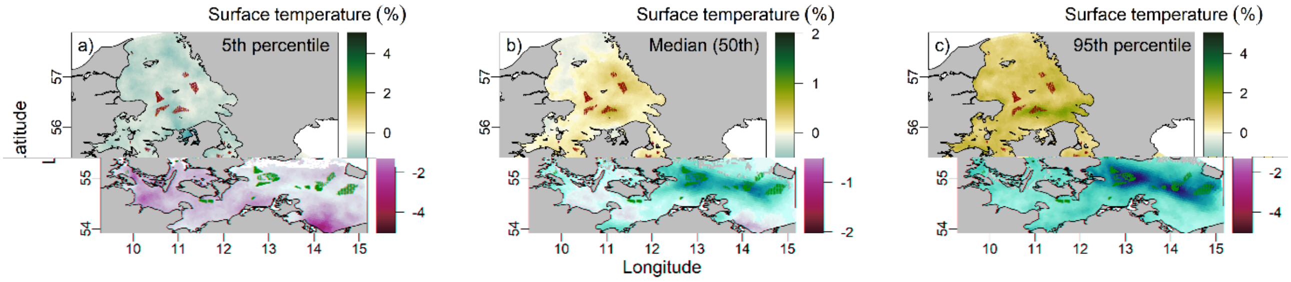

Figure 6.4. Changes in surface temperature for the Y2030 scenario.

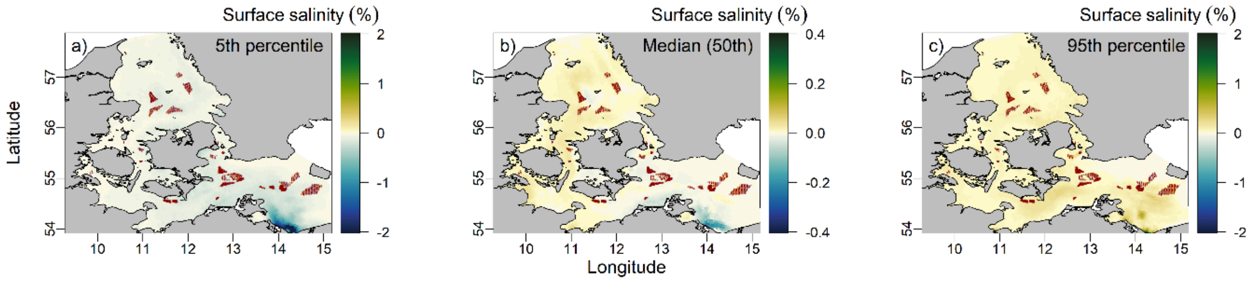

Figure 6.5. Changes in surface salinity for the Y2030 scenario.

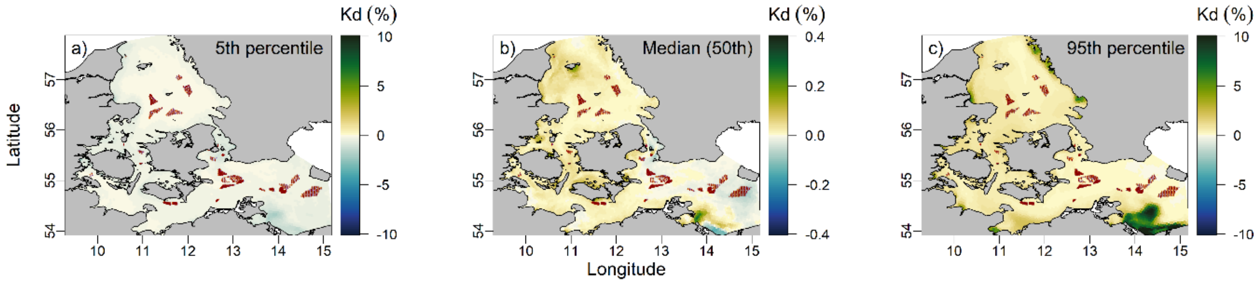

Figure 6.6. Changes in light attenuation (Kd) for the Y2030 scenario.

Biogeochemical variables in the Inner Danish waters:

In the entire model domain, the biogeochemical variables with the highest percentile range (variability) of responses to offshore wind farm development were nitrate concentrations, primary production, Chl *a* concentration and zooplankton production (Table 6.1). Median responses were highest for zooplankton production (-8.1% to 2.9%) and primary production (-5.2% to 1.7%) in Y2030. On median average, the highest response was for Chl *a* (0.043%).

Nitrate concentration mainly increased in coastal areas with decreasing PEA, probably due to a vertical transport of nutrients to the surface layer (Figures 6.7, 6.1). The 95th percentile showed high responses because nitrate concentrations were close to zero during summer. Phosphate concentrations mainly decreased in the open waters and increased outside Oder Lagoon (Figure 6.8). Chl *a* concentration increased in most of the model domain, except for the Arkona basin (Figure 6.9). Primary production showed a high spatial variability with an overall slight decrease (Figure 6.10). In the Arkona Basin, primary production increased, coinciding with the highest increase in stratification and surface temperature. Surface zooplankton biomass decreased in the model domain, except for the Little Belt and outside Oder Lagoon (Figure 6.11). Zooplankton production showed a decrease outside the Oder Lagoon, the Belt Sea and southern Kattegat and an increase in the other areas (Figure 6.12). Bottom oxygen increased in the Belt Sea and Kattegat, whereas there was a decrease outside the Oder Lagoon (Figure 6.13, Table 6.1). Benthos biomass decreased in most of the study areas, probably due to lower bottom temperature affecting growth rates (Figure 6.14).

In the Danish EEZ, the median values and percentile ranges were similar to the entire model domain, except for phosphate and zooplankton biomass influenced by the Oder Lagoon (Table 6.2). Median responses were highest for nitrate (-1.8% to 1.9%), Chl *a* (-1.1% to 1.6%), primary production (-1.4% to 1.4%) and zooplankton production (-1.9% to 3.1%) in Y2030. On average, the highest response was found for Chl *a* (0.057%).

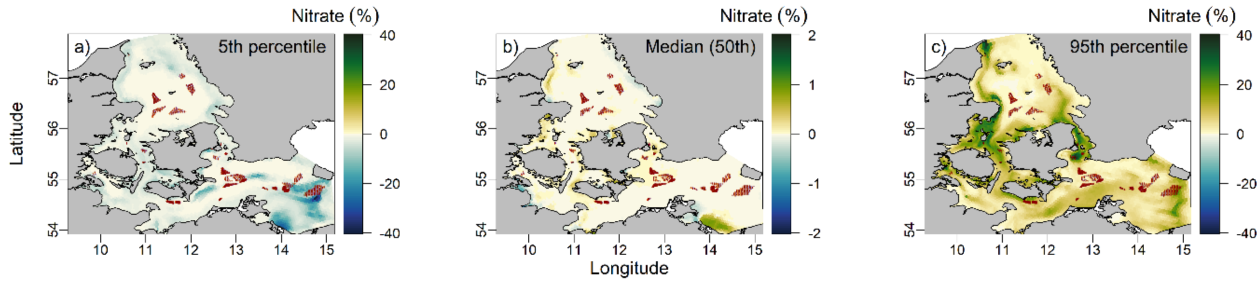

Figure 6.7. Changes in nitrate concentration for the Y2030 scenario.

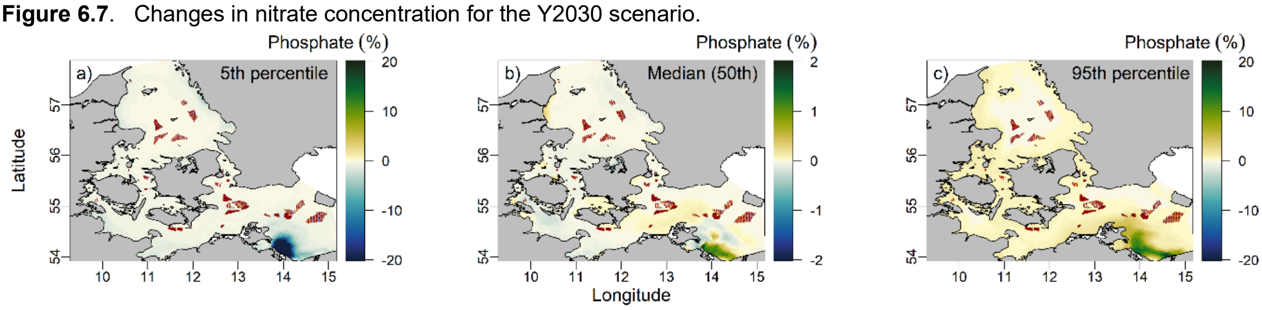

Figure 6.8. Changes in phosphate concentration for the Y2030 scenario.

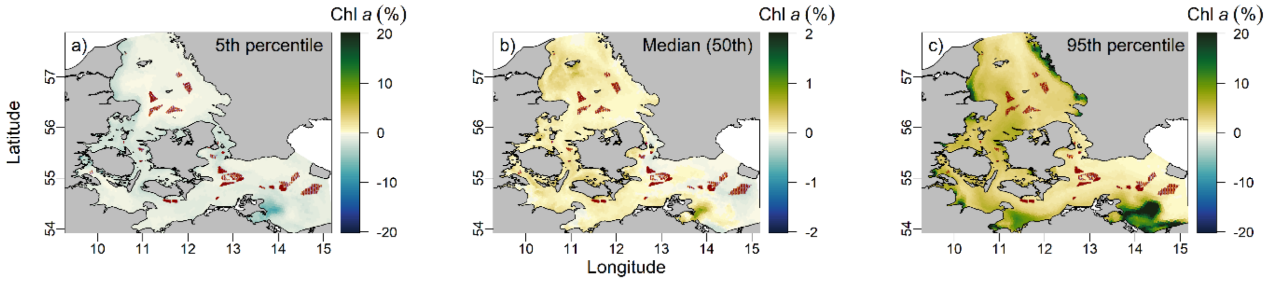

Figure 6.9. Changes in Chl *a* concentration for the Y2030 scenario.

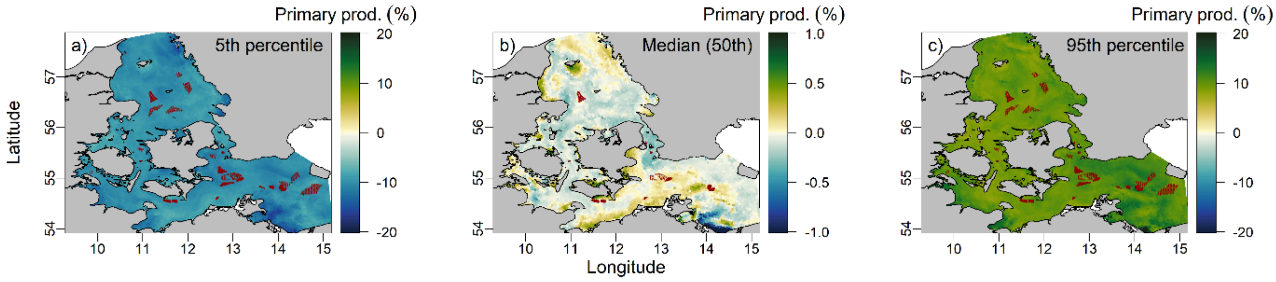

Figure 6.10. Changes in primary production (0-20 m) for the Y2030 scenario.

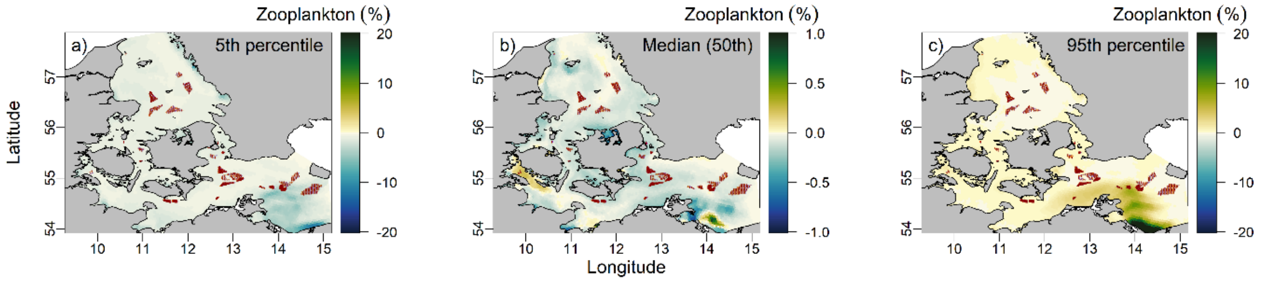

Figure 6.11. Changes in zooplankton biomass for the Y2030 scenario.

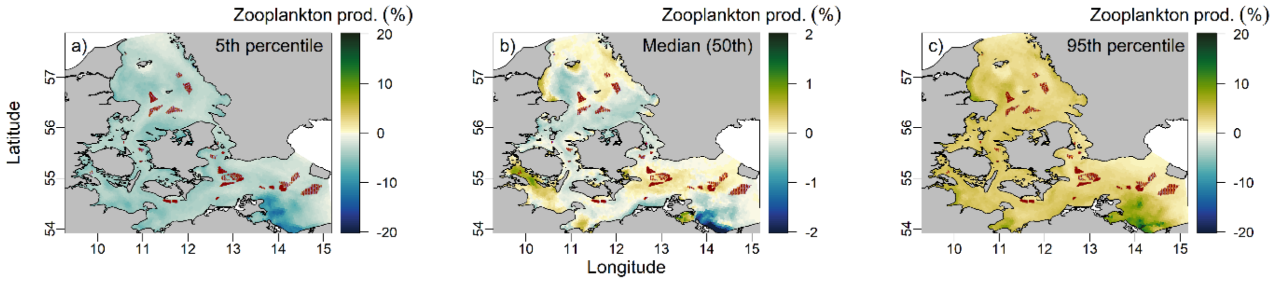

Figure 6.12. Changes in zooplankton production (0-20 m) for the Y2030 scenario.

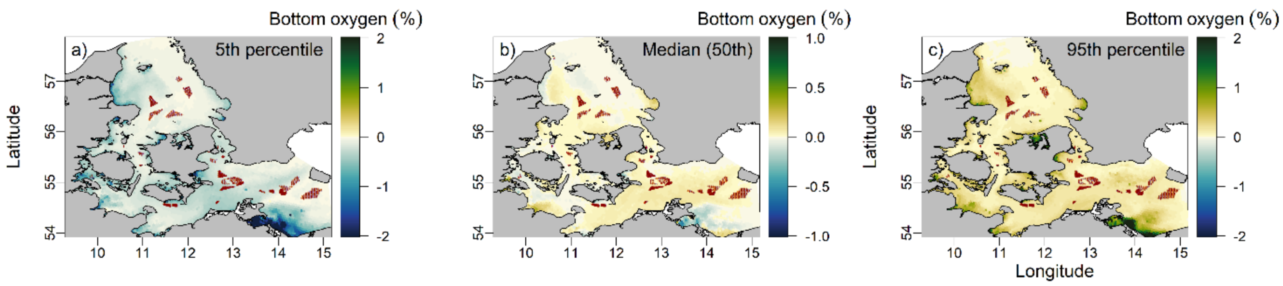

Figure 6.13. Changes in bottom oxygen for the Y2030 scenario.

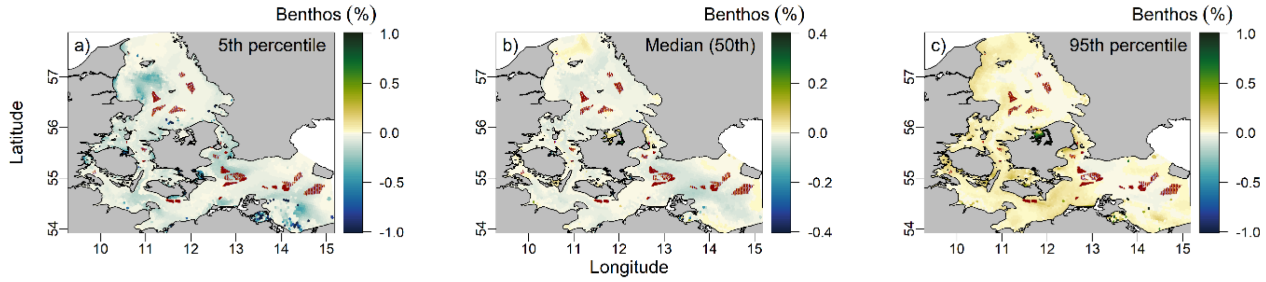

Figure 6.14. Changes in benthos biomass for the Y2030 scenario.

Table 6.2. Summary of model results for the spatial plots shown in the figures 6.1.1-14 for each ecosystem variable in the Danish EEZ of the Inner Danish waters model domain in Y2030 from April to October.

	Y2030			
Danish EEZ, Inner DK waters	**Medians (%) Median / min / max**	**Absolute range (%)**	**Percentiles (%) min / max**	**Absolute range (%)**
Physical variables:				
Stratification index (PEA)	0.002 / -3.3 / 4.1	7	-20.1 / 28.1	48
Surface current speed	-0.003 / -0.5 / 0.2	1	-1.7 / 1.5	3
Bottom stress	-0.004 /-0.6 / 0.3	1	-4.1 / 6.5	11
Surface temperature	0.072 / -0.3 / 1.0	3	-3.3 / 2.7	6
Surface salinity	0.003 / -0.1 / 0.1	0	-0.5 / 0.7	1
Light attenuation Kd	0.029 / -0.1 / 0.2	0	-1.5 / 4.4	6
Biogeochemical variables:				
Surface nitrate	0.010 / -1.8 / 1.9	4	-25.0 / 32.9	93
Surface phosphate	-0.006 / -0.8 / 0.8	2	-2.0 / 3.4	5
Surface Chl *a*	0.057 / -1.1 / 1.6	3	-6.0 / 19.2	25
Primary production (0-20 m)	-0.008 / -1.4 / 1.4	3	-41.6 / 48.3	90
Surface zooplankton biomass	-0.041 / -1.0 / 0.6	2	-6.1 / 2.7	9
Zooplankton production (0-20 m)	0.019 / -1.9 / 3.1	5	-16.2 / 16.1	32
Bottom oxygen	0.004 / -0.3 / 0.5	1	-1.3 / 1.3	3
Benthos biomass	-0.053 / -0.2 / 0.1	0	-0.8 / 0.4	1

6.2 Responses of PEA and primary production inside the offshore wind farms for Y2030

PEA and primary production showed some of the strongest responses to offshore wind farm development in Y2030 (Table 6.1) and are therefore analyzed in more detail. The wind farm areas were defined as the model polygons with at least one wind turbine. Inside the offshore wind farm areas, the seasonal response of PEA showed stronger stratification during summer when the water column is generally more stratified (Figure 6.15a). Primary production showed the highest change in March during the spring bloom and later in July-August (Figure 6.15b). The spring phytoplankton bloom occurred earlier, seen as an increase in the response by the end of February (Figure 6.15b). The seasonal pattern of primary production varied frequently between positive and negative values, demonstrating the complex nature of the response to offshore wind. This pattern could also be seen from the high 5th to 95th percentile range (Table 6.1). In the entire model domain, the PEA only showed a small increase during summer (Figure 6.15c), and the primary production showed lower variability (Figure 6.15d).

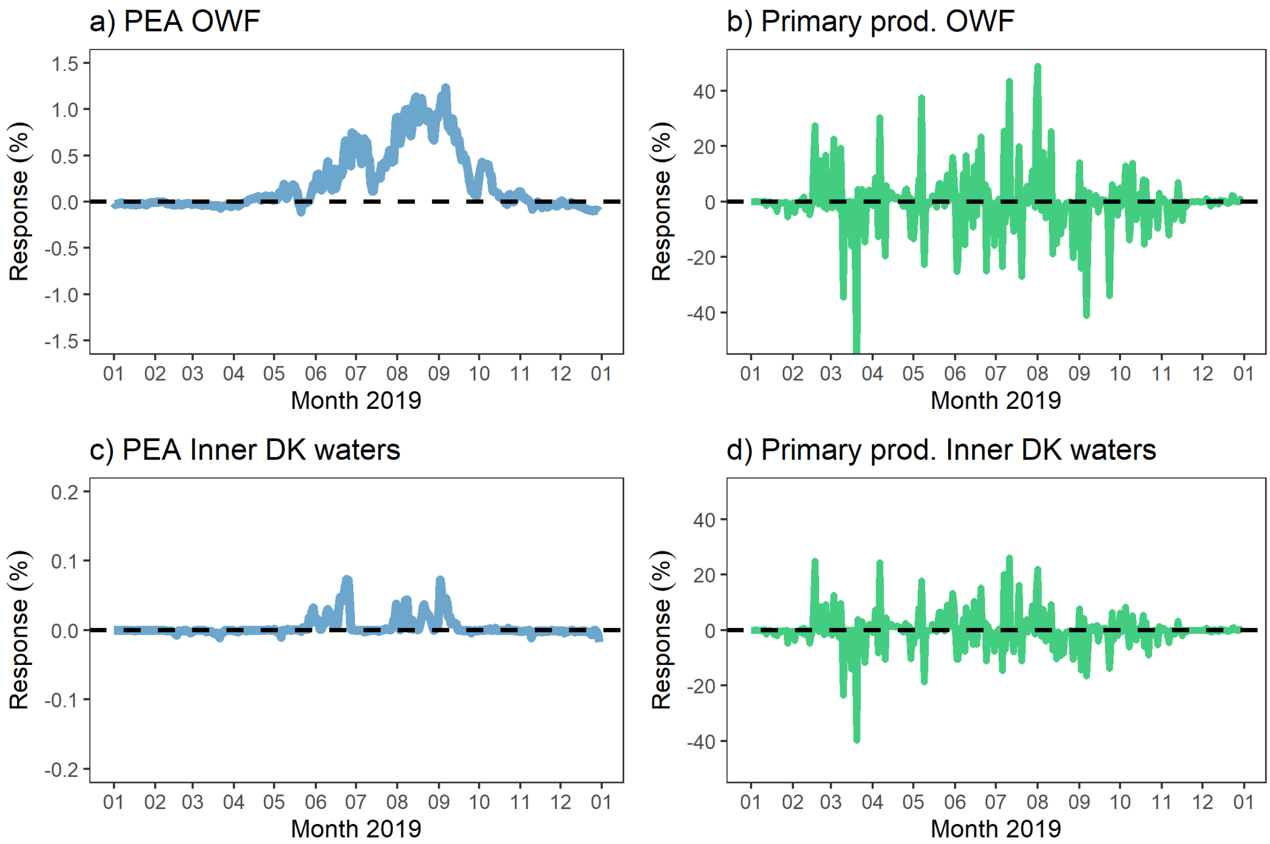

Figure 6.15. Time-series median responses of a) stratification index (PEA) and b) primary production inside offshore wind farm areas and c) stratification index (PEA) and d) primary production in the Inner Danish waters Y2030.

The responses of PEA and primary production in the Inner Danish waters were analyzed against decreases in wind speed (wind wake effect on x-axis) and mean current speed (color scale) in the offshore wind farm areas (Figure 6.16). A decrease in wind speed was expected to give a stronger stratification and reduce primary production (less vertical mixing of nutrients). A faster mean current speed was expected to result in a stronger monopile drag causing less stratification, and more mixing of nutrients to the surface layer and thereby increasing primary production.

In Y2030, PEA was generally found to increase with less wind speed (stronger wind wake) in agreement with our expectations (Figure 6.16a). Only for strong current speeds >0.15 m s^{-1}, PEA decreased with less wind speed (blue color in Figure 6.16a). For decreasing current speeds (color scale), stratification increased due to less monopile mixing as expected. In the North Sea, stratification was also found to increase at low current speeds <0.15 m s^{-1} (Figure 5.16a).

The response of primary production in Y2030 was negative in the offshore wind farms with medium to high current speeds (yellow-green-blue color) as expected due to less wind speed and stronger stratification (Figure 6.16b). In contrast, the offshore wind farms with the strongest change in stratification, lowest current speeds <0.05 m s^{-1} and highest surface temperature increase, showed increased primary production (orange color in Figure 6.16). This area corresponds to the Arkona Basin in the Baltic Sea (Figure 6.4). Hence, in this area increased stratification caused higher surface temperatures that facilitated higher phytoplankton growth rates and recycling of nutrients (Figure 6.16c). In comparison, primary production always increased in the North Sea due to the strong monopile mixing effect at the generally higher current speeds (Figure 5.16b).

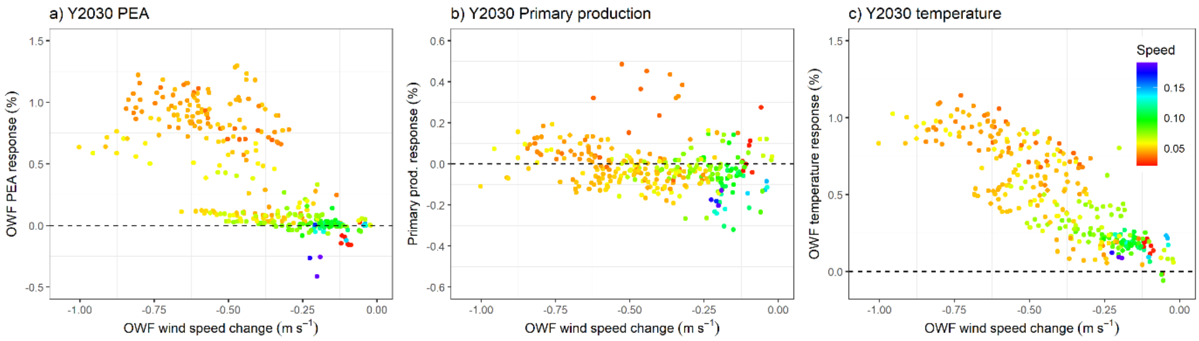

Figure 6.16. Median responses (%) for each model polygon with offshore wind farms (OWF) in Y2030 of a) PEA, b) primary production, and c) surface temperature to wind speed decrease. The mean current speed is shown as color scale, where high current speeds are blue and low speeds are orange.

6.3 Spatial impact index for the entire Inner Danish waters and the Danish EEZ

PEA for the entire model domain of Inner Danish waters:

The spatial impact index is the median change relative to the natural variability. For PEA, the spatial impact index showed responses in the Little Belt and near the offshore wind farms in CURRENT (Figure 6.17a). The impact found in the Little Belt was probably due to far-field effects from the offshore wind farms. In Y2030, the impact index was highest in the Arkona Basin due to a strong wind wake effect (Figures 6.17b).

Primary production for the entire model domain of the Inner Danish waters:

For primary production in CURRENT, the spatial impact index was smoothly distributed in the entire area (Figure 6.18a). Hence, even though there were relatively few wind farms in CURRENT, there were some compensating mechanisms with far-field effects, as seen for the atmospheric model (Figure 1.3b). Higher wind speeds in some areas probably caused mixing of nutrients to the surface layer stimulating primary production. For Y2030, the spatial impact index showed a scattered pattern all over the area (Figure 6.18b). Hence, due to the dominance of the wind wake effect over the monopile mixing effect at low current speeds, the impact on the marine environment was smooth over a long distance.

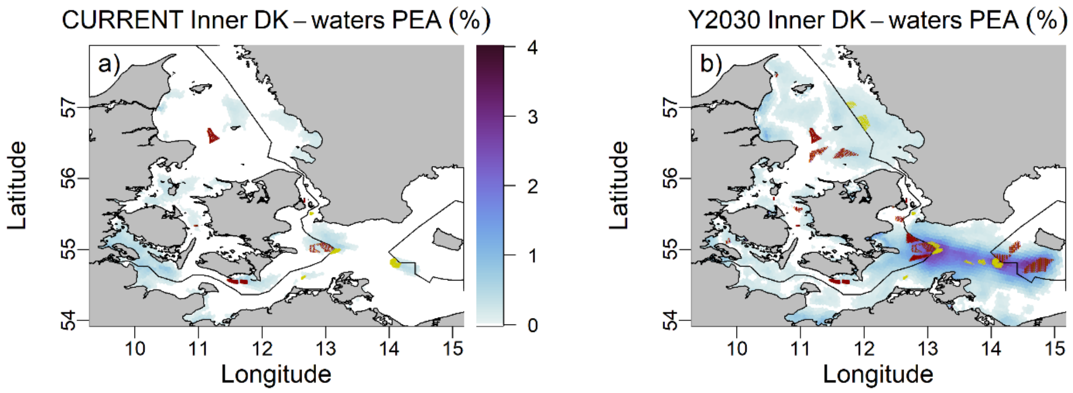

Figure 6.17. PEA spatial impact index (%) for a) CURRENT (max. value=1%), and b) Y2030 (max. value =5%) in the Inner Danish waters. Offshore wind farms are indicated as dark red points in the Danish EEZ and orange points outside Denmark. The DK-EEZ border is shown as a solid black line. Values below 0.1% were omitted in the plots.

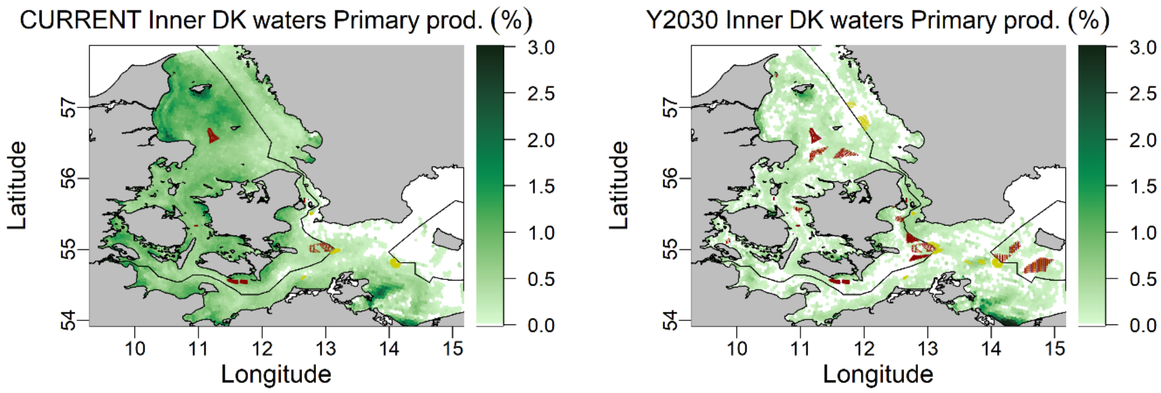

Figure 6.18. Primary production spatial impact index (%) in a) CURRENT (max. value = 4%), and b) Y2030 (max. value = 4%) in the Inner Danish waters. Offshore wind farms are indicated as red points in the Danish EEZ and orange points outside Denmark and the DK-EEZ is shown as a black solid line. Values below 0.1% were omitted in the plots.

The Danish EEZ in the Kattegat and Arkona basin Y2030:

In the Danish EEZ of the Kattegat and Arkona for Y2030, the spatial impact of PEA and primary production showed low and smooth effects over a larger area (Figure 6.19). In the Kattegat, the spatial impact was very low <1% for both PEA and primary production. In the Arkona, the impact was below 4% for PEA and below 1% for primary production. The smooth pattern is due to the wind wake effect.

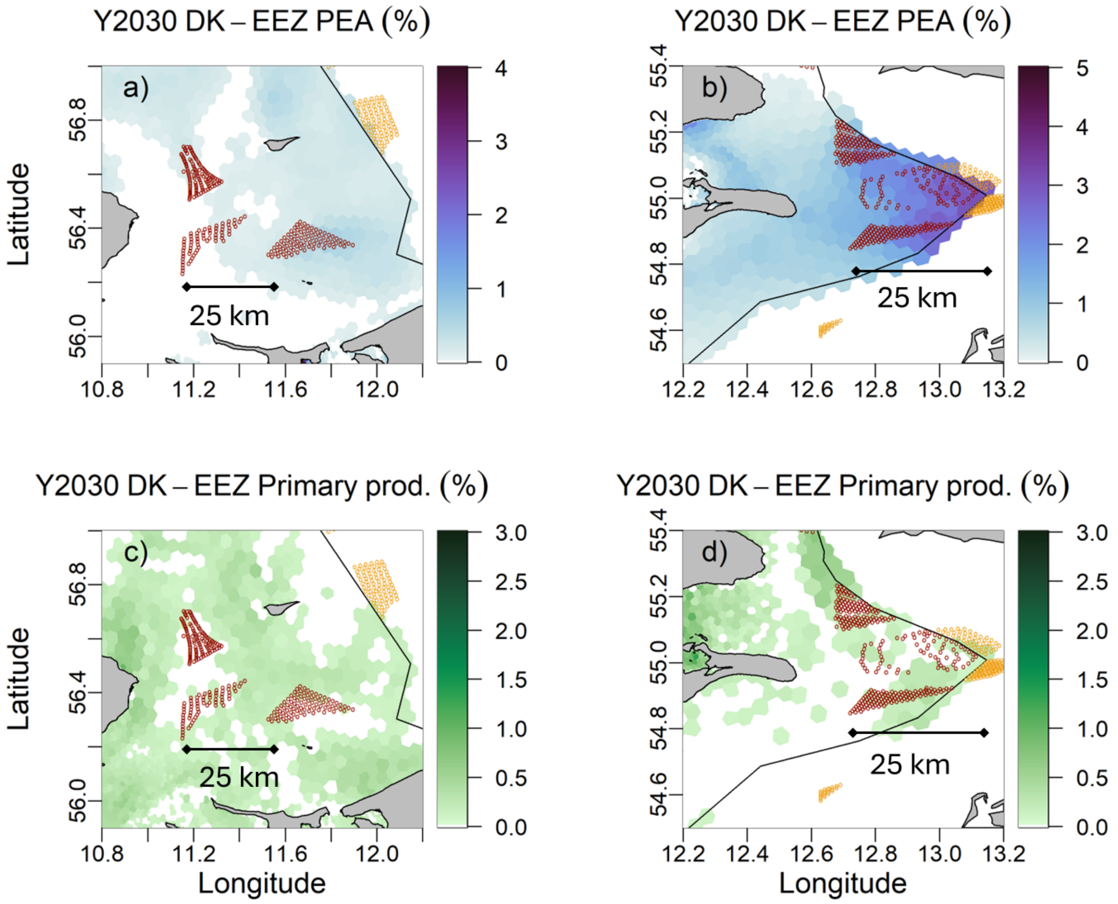

Figure 6.19. Spatial impact index (%) in the Danish EEZ of PEA a) in the Kattegat, b) the Arkona Basin, and of primary production in c) the Kattegat and d) the Arkona Basin. Offshore wind farms are indicated as red points in the Danish EEZ and orange points outside Denmark and the DK-EEZ is shown as a black solid line. Note only changes in the Danish EEZ are shown. Values below 0.1% were omitted in the plots.

6.4 Extreme events

In the eastern Belt Sea, to the west of the island of Bornholm, the model simulations predicted a more significant and consistent impact of wind farms during windy conditions, indicated by a broader increase in stratification (Figure 6.20b), compared to the calm scenario (Figure 6.20a). While the average PEA differences (J m^{-3}) in the eastern Belt Sea were similar across both wind scenarios, the overall range and maximum PEA difference were notably larger under windy conditions (Figure 6.20c, d). In this case, the maximum PEA differences significantly extended PEA differences predicted in the calm scenario (Figure 6.20d). The inner Danish waters are a highly stratified system, and the wake effect from larger offshore wind farm capacities becomes more significant during wind periods with stable atmospheric conditions, leading to a clear enhancement in PEA. This indicates a stronger influence of the wind wakes from the offshore wind farms compared to conditions in the North Sea.

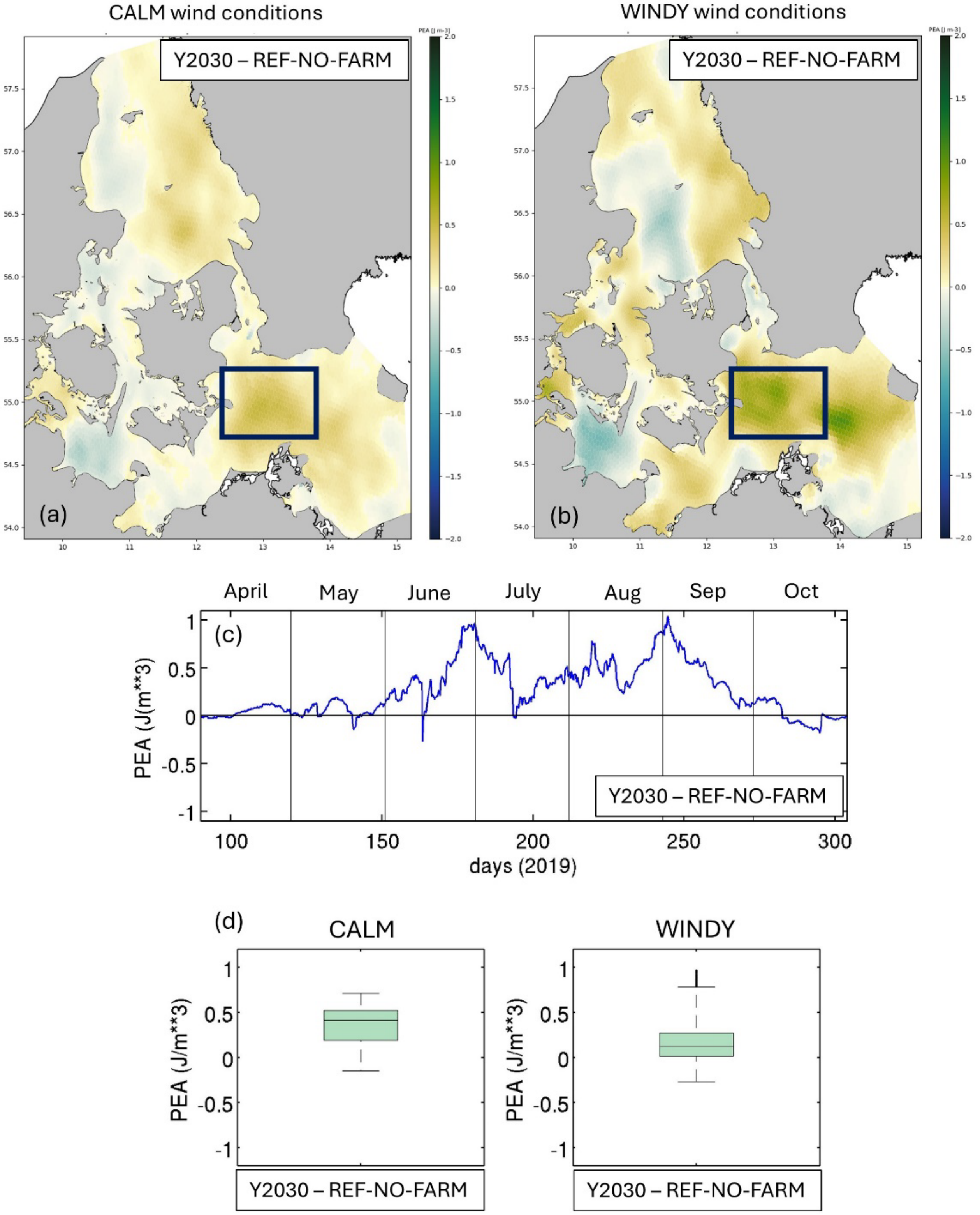

Figure 6.20. Modelled differences of PEA (J m^{-3}) in Inner Danish Waters (eastern Belt Sea) model setup between the Y2030 offshore wind scenario and REF-NO-FARM. (a, b) Spatial maps showing PEA during CALM and WINDY periods. (c) Time series of PEA averaged inside the eastern Belt Sea (blue rectangle in (a) and (b). (d) Box plots of modelled PEA during different wind conditions. Black horizontal bars represent the median. Colored boxes show the 25% and 75% quartiles. Whiskers extend two times the interquartile range indicating the range of values between minimum and maximum across the interquartile. The analysis is based on 3-hourly model output. The CALM and WINDY periods are indicated in Table 1.2

7 Model uncertainties

The formulation of the wind wakes was based on an interactive atmospheric model with realistic wind farm distribution and real turbine sizes that was more accurate than the simpler approach applied in other studies (Table 1.1). However, there was no feedback from the sea to the atmosphere regarding surface fluxes that may affect wind speed and wakes in the atmosphere. It is important to note that interpretation of the scenario results can be complex because the atmospheric forcing not only includes the wind wake effect from offshore wind, but also from the onshore wind farms as well as changes in atmospheric temperature and cloud cover (Hahmann et al. 2025). The atmospheric compensating mechanisms caused an increase in wind speed and mixing of the water column in some local areas outside the offshore wind farms. The mixing effect sometimes caused high responses in the physical and biogeochemical variables, e.g. at the Oder Lagoon, which should be further tested to evaluate potential model bias. The applied wind farm capacity in UK was overestimated in Y2030 and will be reduced in the next version of atmospheric forcing (Hahmann et al. 2025). Hence, this caused some very high effects of PEA and primary production in the UK wind farms.

The formulation of the monopile drag effect depended on the physical shape of the monopiles, including epifauna and the scour protection, and the applied coefficients are therefore uncertain (Christiansen et al. 2023). Further, the relatively coarse resolution of the model may underestimate the wind wake and drag effects compared to small-scale high-resolution modelling. However, the results from a high-resolution FlexSem flume proof-of-concept model demonstrated good agreement between a configuration with an existing monopile, a setup featuring the monopile drag parameterization (but without the monopile), and measurements of the currents downstream of the monopile, obtained from inside the Anholt offshore wind farm (Mohn et al. 2025). Field studies, such as the one reported from the Anholt offshore wind farm, could thus be used to test model parameterizations, but require additional high-quality measurements of currents and stratification relatively close (<<200 m) to the monopile over several months (Mohn et al. 2025).

The scenarios were conducted for one standard year, but the effects may accumulate over years until the system get adjusted to the new impact. Further, assessment of the interannual variations is needed to consolidate the results. The impact was considered as median changes of the summer period from April to October. The spring period showed changes in the timing of the phytoplankton bloom in Y2030 due to changes in stratification/mixing affecting the light availability to primary producers in both study areas. Detritus resuspension is included in the model, but resuspension of inorganic particles is missing and could be important in the tidal areas of the North Sea. At the open boundary between the North Sea and the Inner Danish Waters, some of the results showed a high unexpected effect, e.g.

nitrate, which probably was due to the missing interaction between the two areas. The spatial impact was found to increase with the density of monopiles and wind farm capacity in an area making it difficult to evaluate the sensitivity of an area to one specific wind farm. Future scenarios could include a more equal distribution of identical wind turbines in the allocated areas to offshore wind or by assessing one wind farm at the time.

The FlexSem model set-ups of the North Sea and Inner Danish waters were two relatively new model systems and continued calibration and improvement of physical-biogeochemical processes are foreseen. The models showed good to reasonable performance in comparison with monitoring data. For instance, a new advection-diffusion scheme is under development, which is expected to improve the physical-biogeochemical gradients from coast to open waters.

8 Discussion

The two study areas are very different with respect to the level of stratification and current speed. The North Sea is seasonally stratified, with strong current speeds and mixing in the tidal areas. The Inner Danish waters are strongly stratified most of the year, with lower current speeds compared to the North Sea. The current situation (year 2021) and future developments (year 2030) of offshore wind were shown to impact hydrodynamics and the biogeochemical environment differently in the two areas due to the combined effects of wind wakes and monopile mixing. Over time, advection and lateral transport cause the anomalies to spread over a large scale in the affected areas. The stratification index, nutrient concentrations and primary production responded most strongly to offshore wind with respect to variability among the considered variables in both areas.

In the North Sea, the monopile mixing effect generally dominated the response of PEA due to the higher current speeds and caused lower stratification inside the offshore wind farms. In the Inner Danish waters, the wind wake effect dominated due to lower current speeds and caused stronger stratification both outside and within the offshore wind farms. The monopile mixing effect was found to dominate over the wind wake effect at water current speeds >0.15 m s^{-1} in both study areas. The spatial gradients between areas with and without offshore wind farms were generally stronger in the North Sea than in the Inner Danish waters, showing a smoother pattern. A previous offshore wind farm model study in the Baltic Sea also showed large-scale smooth patterns of temperature and salinity changes (Arneborg et al. 2024). Stratification for the Danish EEZ showed a median change of -8.1% to 1.3% in the North Sea (Table 5.2) and a median change in the Inner Danish waters of -3.3% to 4.1% (Table 6.2). However, the daily variability showed much higher values according to the 5^{th} and 95^{th} percentiles of ±17-28% in both EEZs.

Primary production increased within the offshore wind farms in the North Sea due to the monopile mixing causing vertical transport of nutrients to the productive surface layer. In the Inner Danish waters, primary production mainly decreased both outside and within the offshore wind farms due to stronger stratification and less input of nutrients to the surface. However, in offshore wind farms with the strongest increase in stratification and surface temperature, primary production increased due to faster phytoplankton growth and recycling of nutrients. Primary production in the Danish EEZ showed a median change of -0.5% to 1.6% in the North Sea (Table 5.2) and a median change of -1.4% to 1.4% the Inner Danish waters (Table 6.2). However, the upper and lower percentiles showed higher daily changes of ±7 and ±48% in the EEZ of the North Sea and the inner Danish waters, respectively.

The onset of the spring phytoplankton bloom is governed by the increasing light irradiance. Stabilization of the water column affects bloom development indirectly by reducing the depth of the upper mixed layer and, hence, the vertical mixing of phytoplankton below the critical depth for photosynthesis. The bloom was delayed in the offshore wind farm areas in the North Sea due to higher mixing reducing the light availability to phytoplankton (Figure 5.15b). The same effect was found in another North Sea model study of offshore wind farm effects (van Duren et al. 2021). The spring phytoplankton bloom was, on the other hand, initiated earlier in the offshore wind farm in the Inner Danish waters, probably due to reduced mixing below the photic zone (Fig.6.15b).

Surface temperature was found to increase in areas with increasing stratification, on median average 0.02°C (max=0.12°C) in the entire North Sea and 0.001°C (max=0.02°C) in the entire Inner Danish waters. A previous study including only the wind wake effect found a temperature increase of 0.002 to 0.05°C in the North Sea (Christiansen et al. 2022). Another study in the North Sea found a decrease in temperature due to the monopile drag effect, but did not consider the wake effect (van Duren et al. 2021). In the Baltic Sea, a study found that surface temperatures mainly increased (<0.1°C), but to a lesser extent than for bottom waters (Arneborg et al. 2024). The found temperature increases are small, but add to the predicted increase of 2-3°C from global warming (Kristiansen et al. 2023).

The found spatial- and temporal changes in pelagic productivity could have implications for food availability for higher trophic levels. In the North Sea, productivity increased in the offshore wind farm areas but decreased in the more open stratified waters with existing lower primary production (Figure A1.4). Hence, offshore wind farms may strengthen the occurring spatial gradients of productivity between coastal and open waters (Daewel et al. 2022).

The response in bottom oxygen (hypoxia) is complex, since oxygen consumption would decrease with lower pelagic production and lower bottom temperature, whereas the vertical ventilation would decrease with a stronger stratification leading to more oxygen deficiency in the bottom waters. The model only showed small changes (<2.9%) in bottom oxygen in both areas, but the response may increase if running more years due to cumulative effects in the sediment and bottom waters.

The spatial impact index (%) was estimated for stratification (PEA) and primary production as the absolute median change relative to the natural variability (standard deviation). For the Danish EEZ, the spatial impact index was relatively low with <20% and <5% in the North Sea and the Inner Danish waters, respectively, compared to the neighboring countries. The lower impact in the Danish EEZ was due to lower wind farm capacity and density of monopiles in the scenarios and, in some cases, lower current speed. Outside the Danish EEZ, there were strong responses to offshore wind in the English Channel, off the Scotland coast and outside Oder Lagoon. The English Channel showed indications of cumulative impacts over a larger area in between the wind farms, mainly due to monopile mixing at the high current speeds. Outside the Oder Lagoon, the increase in wind speed due to compensation atmospheric mechanisms caused some strong effects on the stratification and biogeochemical environment, but further testing is needed to verify this result.

For the Danish EEZ in the North Sea, the impact range was less than 5 km away from the wind farms. In the EEZ in the Inner Danish waters, the spatial impact was very smooth, and it was not possible to estimate an impact range. For both waters, there were additional diffuse changes compared to the reference spread across the area that cannot be assigned to one specific wind park.

The present study shows the importance of including both the wind wake effect and the monopile drag effect since they are opposing forces, making the responses highly complex in space and time in marine waters. Further, the modeling study emphasizes the critical need to consider the specific hydrodynamic and biogeochemical conditions of an area when evaluating the impacts of offshore wind farms. Models can be used to test different upscaling scenarios and wind farm configurations to minimize the impact on the marine environment. The model results showed that different hydrodynamic regimes determine the type of response (positive or negative), but that high numbers of wind turbines per area can cause cumulative effects and increase the magnitude of ecosystem responses. Hence, larger turbines with high distance between them would cause less effects than many smaller turbines with small distance.

The found changes in productivity and temperatures could potentially affect higher trophic levels. One next step could be to couple the output of the hydrodynamic-biogeochemical models to bivalves and seaweed and higher trophic levels, such as marine mammals, fish and birds, to get a full end-to-end approach of food web effects from offshore wind farm development. Sessile organisms, such as mussels and seaweed colonizing the turbines, may also contribute to changes in nutrient cycling, Chl *a* concentrations and carbon deposition (Maar et al. 2009, De Borger et al. 2021). Another model development could be to include colonizing species on the turbines with feed-backs to the biogeochemical model and higher trophic levels.

9 References

Arneborg L, Pemberton NG, Axell L, Saraiva S, Mulder E, Fredriksson S (2024) Hydrographic effects in Swedish waters of future offshore wind power scenarios. REPORT OCEANOGRAPHY No 77. Department of Research and Development, SMHI.

Burchard H, Petersen O, Rippeth TP (1998) Comparing the performance of the Mellor-Yamada and the k-epsilon two-equation turbulence models. J Geophys Res-Oceans 103:10543-10554

Cazenave PW, Torres R, Allen JI (2016) Unstructured grid modelling of offshore wind farm impacts on seasonally stratified shelf seas. Prog Oceanogr 145:25-41

Christiansen N, Carpenter JR, Daewel U, Suzuki N, Schrum C (2023) The large-scale impact of anthropogenic mixing by offshore wind turbine foundations in the shallow North Sea. Frontiers in Marine Science 10

Christiansen N, Daewel U, Djath B, Schrum C (2022) Emergence of Large-Scale Hydrodynamic Structures Due to Atmospheric Offshore Wind Farm Wakes. Frontiers in Marine Science 9

Ciavatta S, Brewin RJW, Skákala J, Polimene L, de Mora L, Artioli Y, Allen JI (2018) Assimilation of Ocean-Color Plankton Functional Types to Improve Marine Ecosystem Simulations. J Geophys Res Oceans 123:834-854

Crocker R, Maksymczuk J, Mittermaier M, Tonani M, Pequignet C (2020) An approach to the verification of high-resolution ocean models using spatial methods. Ocean Sci 16:831-845

Daewel U, Akhtar N, Christiansen N, Schrum C (2022) Offshore wind farms are projected to impact primary production and bottom water deoxygenation in the North Sea. Communications Earth & Environment 3:292

De Borger E, Ivanov E, Capet A, Braeckman U, Vanaverbeke J, Grégoire M, Soetaert K (2021) Offshore Windfarm Footprint of Sediment Organic Matter Mineralization Processes. Frontiers in Marine Science 8

Edwards KP, Barciela R, Butenschön M (2012) Validation of the NEMO-ERSEM operational ecosystem model for the North West European Continental Shelf. Ocean Sci 8:983-1000

Eilola K, Gustafsson BG, Kuznetsov I, Meier HEM, Neumann T, Savchuk OP (2011) Evaluation of biogeochemical cycles in an ensemble of three state-of-the-art numerical models of the Baltic Sea. J Mar Syst 88:267-284

Energistyrelsen (2024a) Notat om scenarier for havvindudbygning frem mod 2030.

Energistyrelsen (2024b) Notat om scenarier for havvindudbygning frem mod 2050.

Hahmann AN, Imberger M, Fischereit J, Alonso-de-Linaje NG, Badger J (2025) Environmental Mapping and Screening of the Offshore Wind Potential in Denmark. Sensitivity mapping: Wind, DTU Public report number DTU E-0255 2025.

Kristiansen T, Butenschön M, Peck MA (2023) Statistically Downscaled CMIP6 Ocean Variables for European Waters. In Review at Scientific Reports. https://doi.org/10.21203/rs.3.rs-3249663/v1.

Larsen J (2024) FlexSem source code [Software]. Zenodo. https://doi.org/10.5281/zenodo.13268690.

Larsen J, Maar M, Mohn C, Pastor A (2020) A versatile marine modelling tool applied to arctic, temperate and tropical waters. PLOS ONE 15:e0231193

Lenhart HJ, Mills DK, Baretta-Bekker H, van Leeuwen SM, van der Molen J, Baretta JW, Blaas M, Desmit X, Kuhn W, Lacroix G, Los HJ, Menesguen A, Neves R, Proctor R, Ruardij P, Skogen MD, Vanhoutte-Brunier A, Villars MT, Wakelin SL (2010) Predicting the consequences of nutrient reduction on the eutrophication status of the North Sea. J Mar Syst 81:148-170

Li X, Chi L, Chen X, Ren Y, Lehner S (2014) SAR observation and numerical modeling of tidal current wakes at the East China Sea offshore wind farm. J Geophys Res Oceans 119:4958-4971

Lindström G, Pers C, Rosberg J, Strömqvist J, Arheimer B (2010) Development and testing of the HYPE (Hydrological Predictions for the Environment) water quality model for different spatial scales. Hydrology Research 41:295-319

Lu Z, Li G, Liu Z, Wang L (2022) Offshore wind farms changed the spatial distribution of chlorophyll-a on the sea surface. Frontiers in Marine Science 9

Mohn C, Larsen J, Maar M (2025) Ocean currents and water mass properties inside the Anholt Offshore Wind Farm (Kattegat, Denmark). DCE technical report, in preparation.

Maar M, Bolding K, Petersen JK, Hansen JLS, Timmermann K (2009) Local effects of blue mussels around turbine foundations in an ecosystem model of Nysted off-shore wind farm, Denmark. J Sea Res 62:159-174

Maar M, Larsen J, Dahl K, Riemann B (2018) Modelling the environmental impacts of future offshore fish farms in the inner Danish waters. Aquaculture Environment Interactions 10:115-133

Maar M, Larsen J, Schourup-Kristensen V (2022) FlexSem Biogeochemical model with mussel farming V10. Zenodo

Maar M, Larsen J, von Thenen M, Dahl K (2020) Site selection of mussel mitigation cultures in relation to efficient nutrient compensation of fish farming. Aquaculture Environment Interactions 12:339-358

Maar M, Markager S, Madsen KS, Windolf J, Lyngsgaard MM, Andersen HE, Møller EF (2016) The importance of local versus external nutrient loads for Chl a and primary production in the Western Baltic Sea. Ecol Model 320:258-272

Maar M, Møller EF, Larsen J, Madsen KS, Wan ZW, She J, Jonasson L, Neumann T (2011) Ecosystem modelling across a salinity gradient from the North Sea to the Baltic Sea. Ecol Model 222:1696-1711

Maar M, Schourup-Kristensen V, Larsen J, Ishimwe A, Mohn C (2025) FlexSem hydrodynamic-biogeochemical model North Sea [Software]. Zenodo. https://doi.org/10.5281/zenodo.15358807.

Neumann T, Radtke H, Cahill B, Schmidt M, Rehder G (2022) Non-Redfieldian carbon model for the Baltic Sea (ERGOM version 1.2) – implementation and budget estimates. Geosci Model Dev 15:8473-8540

Radach G, Moll A (2006) Review of three-dimensional ecological modelling related to the North Sea shelf system. Part II: Model validation and data needs. Oceano 44:1-60

Rennau H, Schimmels S, Burchard H (2012) On the effect of structure-induced resistance and mixing on inflows into the Baltic Sea: A numerical model study. Coastal Engineering 60:53-68

Schourup-Kristensen V, Mohn C, Larsen J, Stæhr PA, Buur H, Dahl K, Maar M (2024) Spredningsveje for ikke-hjemmehørende arter i Nordsøen. En modelanalyse. Aarhus Universitet, DCE – Nationalt Center for Miljø og Energi, 44 s - Teknisk rapport nr 307

Schrum C, Alekseeva I, St John M (2006) Development of a coupled physical-biological ecosystem model ECOSMO - Part I: Model description and validation for the North Sea. J Mar Syst 61:79-99

Schultze LKP, Merckelbach LM, Horstmann J, Raasch S, Carpenter JR (2020) Increased Mixing and Turbulence in the Wake of Offshore Wind Farm Foundations. J Geophys Res Oceans 125:e2019JC015858

Simpson JH, Bowers D (1981) Models of Stratification and Frontal Movement in Shelf Seas. Deep-Sea Research Part A-Oceanographic Research Papers 28:727-738

Smagorinsky J (1963) General circulation experiments with the primitive equations. Monthly Weather Review 91:99-164

Smith SD, Banke EG (1975) Variation of the sea surface drag coefficient with wind speed. Quarterly Journal of the Royal Meteorological Society 101:665-673

Svendsen LM, Tornbjerg H (2022) Assessment of sources of nutrient inputs to the Baltic Sea in 2017. Helsinki Commission-HELCOM. Baltic Sea Environment Proceedings No. 187 https://helcom.fi/wp-content/uploads/2022/12/PLC-7-Assessment-of-sources-of-nutrient-inputs-to-the-Baltic-Sea-in-2017.pdf.

Thomas DN, Baumann MEM, Gleitz M (1992) Efficiency of carbon assimilation and photoacclimation in a small unicellular Chaetoceros species from the Weddell Sea (Antarctica): influence of temperature and irradiance. J Exp Mar Biol Ecol 157:195-209

van de Wolfshaar KE, Daewel U, Hjøllo SS, Troost TA, Kreus M, Pätsch J, Ji R, Maar M (2021) Sensitivity of the fish community to different prey fields and importance of spatial-seasonal patterns. Mar Ecol Prog Ser 680:79-95

van Duren L, zijl F, van Kessel T, van Zelst VTM, Vilmin L, van der Meer J, Aarts GM, van der Molen J, Soetaert K, Minns AW (2021) Eosystem effects of large up-scaling of offshore wind on the North Sea - a synthesis. Deltares.

van Leeuwen S, Tett P, Mills D, van der Molen J (2015) Stratified and nonstratified areas in the North Sea: Long-term variability and biological and policy implications. J Geophys Res Oceans 120:4670-4686

van Leeuwen SM, Lenhart H-J, Prins TC, Blauw A, Desmit X, Fernand L, Friedland R, Kerimoglu O, Lacroix G, van der Linden A, Lefebvre A, van der Molen J, Plus M, Ruvalcaba Baroni I, Silva T, Stegert C, Troost TA, Vilmin L (2023) Deriving pre-eutrophic conditions from an ensemble model approach for the North-West European seas. Frontiers in Marine Science 10

Volker PJH, Hahmann AN, Badger J, Jørgensen HE (2017) Prospects for generating electricity by large onshore and offshore wind farms. Environ Res Lett 12:034022

Warner JC, Sherwood CR, Arango HG, Signell RP (2005) Performance of four turbulence closure models implemented using a generic length scale method. Ocean Model 8:81-113

Windolf J, Thodsen H, Troldborg L, Larsen SE, Bøgestrand J, Ovesen NB, Kronvang B (2011) A distributed modelling system for simulation of monthly runoff and nitrogen sources, loads and sinks for ungauged catchments in Denmark. J Environ Monit 13:2645-2658

10 Appendix A. Model validation and quality assurance

Validation of the applied models

10.1 Applied metrics

Model results of water level, temperature, salinity, nitrate, phosphate, Chl *a* and oxygen were validated against monitoring data. The correlation coefficient, *R*, was estimated using Pearson's with a type 2 error of 5%. A high correlation coefficient indicates a good agreement between observations and model results. *R* is sensitive to extreme values and seasonal timing, but not to a consistent bias between observations and model.

A cost function, *CF*, was used to assess the model performance:

$$CF = \sum_{i=1}^{N} \frac{|(M_i - O_i)|}{N \times STD_O} \qquad \text{(eq. 1)}$$

Where *N*= number of data points, *M*= model data, *O*= observational data, STD_O = standard deviation of the observations (Radach & Moll 2006). According to the *CF* value, the model performance can be good (*CF* <1), reasonable (*CF* =1-2) or poor (*CF* >2) (Eilola et al. 2011). Hence, the model results are interpreted as good if the model mean deviates with less than plus or minus one standard deviation from the observed mean. The *CF* is sensitive to extreme values and consistent bias.

The normalized standard deviation, *nSTD*, was estimated as the ratio between the standard deviations of model data (STD_M) and observational data:

$$nSTD = \frac{STD_M}{STD_O} \qquad \text{(eq. 2)}$$

The results are interpretated as good if the *nSTD* is within ±1.25 (Eilola et al. 2011). The *nSTD* is a measure of the variability between observations and model results and is sensitive to extreme values.

10.2 North Sea validation

Model results from REF-NO-FARM were compared with monitoring data from 2019. Model performance of sea surface height, surface and bottom temperature and salinity for the open water stations in the North Sea were reported in a previous study (Schourup-Kristensen et al. 2024). Model results of sea surface height were compared with remote sensing data from 12 stations and with measurements from 6 stations on the west and east coasts of the North Sea. Surface and bottom temperature and salinity were compared against ICES data from 16 stations in the western part and 12 stations in the eastern part. In summary, the tested physical variables all showed a good to reasonable model performance according to the cost function (Schourup-Kristensen et al. 2024).

In the present study, we included 19 Danish open water stations for CTD measurements and 23 Danish open water stations measuring water quality, all sampled twice per year in February and September (Figure A1.1). In addition, two coastal stations, RIB and RKB, sampled almost weekly with 45 samples per year, were included in the analysis. The measured variables were temperature, salinity, nitrate, phosphate, Chlorophyll *a* (Chl *a*) and oxygen. All variables at the open water stations showed high correlations and good model performance (Table A1.1). Time-series data from RKB and RIB confirmed a good agreement between model and observations of surface temperature and salinity (Table A1.2, Figure A1.2). At RIB, surface salinity was overestimated and nitrate underestimated during spring and early winter because of too little outflow in the model from the less saline Wadden Sea. Likewise, the nSD was too low for nitrate due to the missing outflow from the Wadden Sea. Nitrate, phosphate, Chl *a* and oxygen all showed a high correlation between model results and observations and the cost functions indicated good model performance.

Figure A1. 1. Map of monitoring stations used for model validation. The stations were 19 open water CTD stations (red circles), 23 water quality stations (green stars) both sampled twice per year, and two coastal stations, RKB (orange point) and RIB (green point) sampled 45 times per year. The freshwater sources are shown as blue circles.

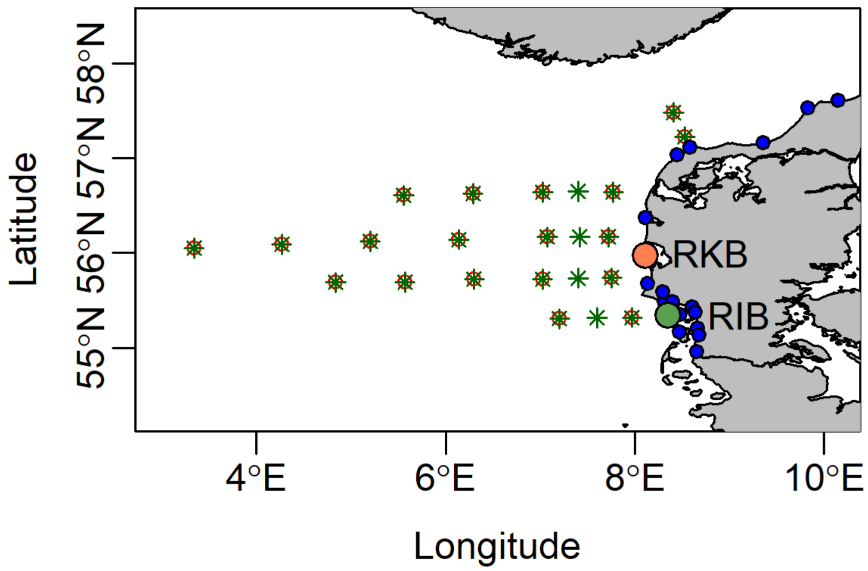

Table A1.1. Model validation against surface monitoring data from open water stations in the Danish North Sea.

Variable	unit	*N*	*R*	*p*	*nSD*	*CF*
Temperature	°C	31	0.99	<0.01	1.03	0.04
Salinity	psu	31	0.60	<0.01	0.96	0.65
Nitrate	mmol m^{-3}	47	0.83	<0.01	2.01	1.87
Phosphate	mmol m^{-3}	47	0.85	<0.01	1.29	0.02
Chl *a*	mg m^{-3}	47	0.89	<0.01	1.19	0.34
Oxygen	mmol m^{-3}	46	0.99	<0.01	1.00	0.03

Table A1.2. Model validation against time-series of monitoring data from RIB and RKB coastal stations.

Variable	unit	*N*	*R*	*p*	*nSD*	*CF*
Temperature	°C	44	0.98	<0.01	1.02	0.04
Salinity	psu	44	0.63	<0.01	1.02	0.94
Nitrate	mmol m^{-3}	45	0.76	<0.01	0.50	0.19
Phosphate	mmol m^{-3}	45	0.78	<0.01	0.80	0.35
Chl *a*	mg m^{-3}	45	0.78	<0.01	0.84	0.11
Oxygen	mmol m^{-3}	45	0.84	<0.01	1.14	0.32

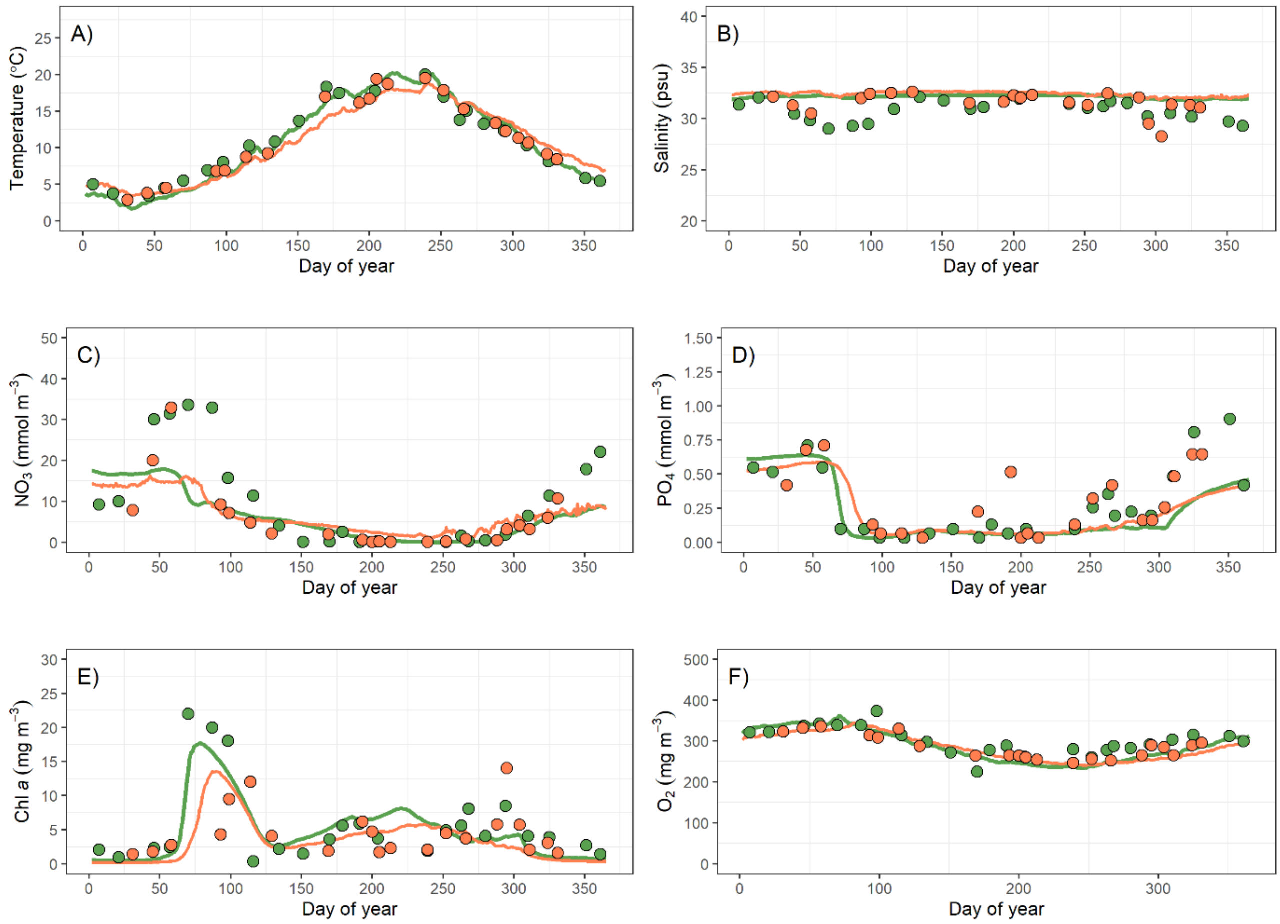

Figure A1.2. Comparison of model results (solid lines) versus monitoring data (points) from the two coastal stations RIB (green) and RKB (orange) of A) surface temperature, B) surface salinity, C) nitrate concentration, D) phosphate concentration, E) surface Chl *a* concentration, and F) surface oxygen concentration in 2019.

10.3 North Sea physical and biogeochemical spatial patterns

Model means (April to October) of the physical and biogeochemical variables in REF-NO-FARM are shown in figures A1.3 and A1.4, respectively. In the English Channel, stratification is low, current speeds and bottom stress are high due to the tides, and temperature and salinity are high due to Atlantic water inflow. In the central North Sea, stratification is stronger and current speed and bottom stress lower. The German Bight shows strong spatial gradients of all physical variables from the coast to the more open waters.

The south-eastern part shows generally higher nutrient concentrations, Chl *a* concentrations, zooplankton biomass, benthos biomass, primary- and zooplankton production. The English Channel and the central part show lowest benthos biomass, plankton biomass and production. The simulated patterns are similar to previous model results for the North Sea (Schrum et al. 2006, Edwards et al. 2012, van de Wolfshaar et al. 2021)

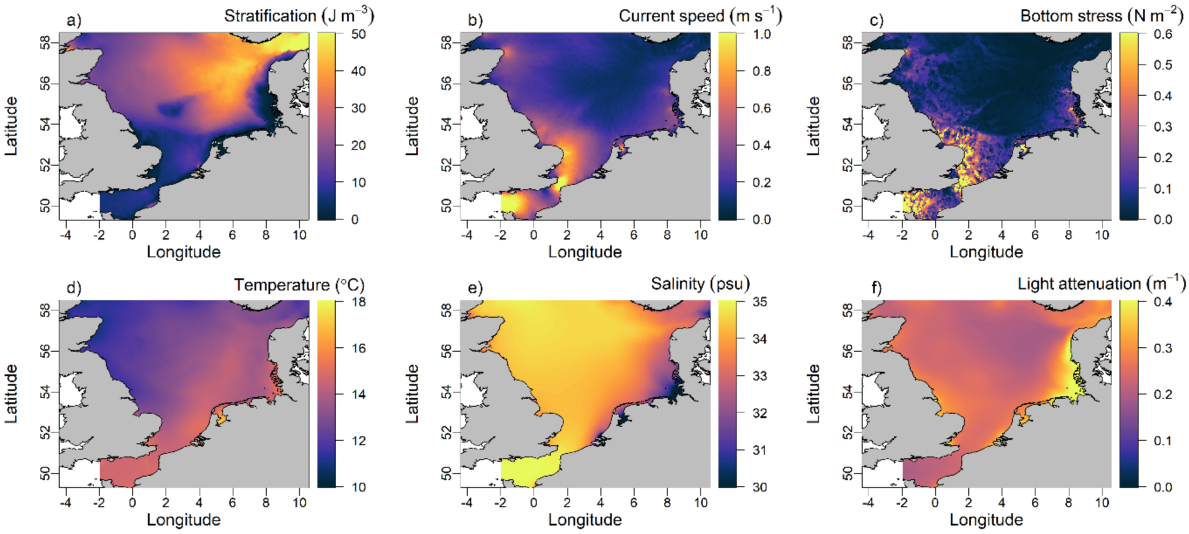

Figure A1.3. Means (April to October 2019) of physical variables, a) stratification PEA, b) current speed, c) bottom stress, d) temperature, e) salinity, f) light attenuation.

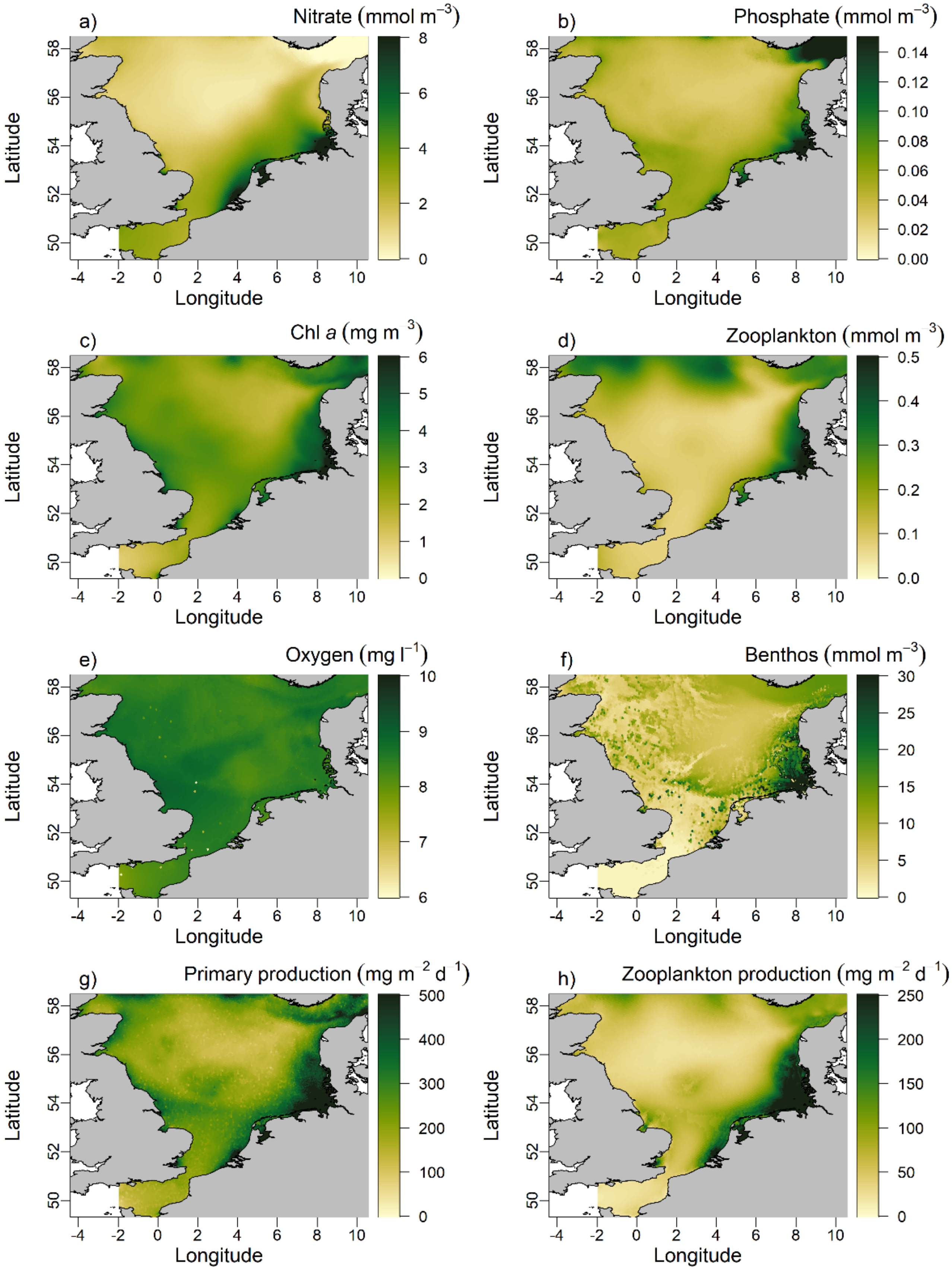

Figure A1.4. Means (April to October 2019) of biogeochemical variables, a) nitrate, b) phosphate, c) Chl a, d) zooplankton, e) oxygen, f) benthos, g) primary production, and h) zooplankton production.

10.4 Inner Danish waters validation

Model results in REF-NO-FARM from two stations, the Great Belt and the Øresund, in the Inner Danish waters were compared with monitoring data from 2019. The two stations were chosen because they are located at two important sites for the water exchange between the Kattegat and the Baltic Sea. The tested variables were surface temperature, salinity, nitrate, phosphate, Chl *a*, and surface- and bottom oxygen. All variables at the open water stations showed high correlations (Table A1.3). The cost function and the normalized standard deviation also indicated a good model performance except for nitrate. The model underestimated nitrate concentration in March and November, where monitoring data showed a peak in the Øresund (Figure A1.5). Surface temperature showed a good fit to measurements, whereas salinity was too high during the summer months in the Great Belt. Phosphate concentrations were generally too high in summer, and the autumn phytoplankton bloom was too low in the model. Overall, the main seasonal characteristics were reproduced by the model (Figure A1.5).

Table A1.3. Model validation against surface monitoring data for two stations in the Inner Danish waters.

Variable	unit	*N*	*R*	*p*	*nSD*	*CF*
Temperature	°C	46	0.99	<0.01	1.03	0.04
Salinity	psu	46	0.60	<0.01	0.96	0.65
Nitrate	mmol m^{-3}	48	0.83	<0.01	2.01	1.87
Phosphate	mmol m^{-3}	48	0.85	<0.01	1.29	0.02
Chl *a*	mg m^{-3}	49	0.89	<0.01	1.19	0.34
Oxygen surf	mg L^{-1}	46	0.99	<0.01	1.00	0.03
Oxygen bottom	mg L^{-1}	46	0.99	<0.01	1.00	0.03

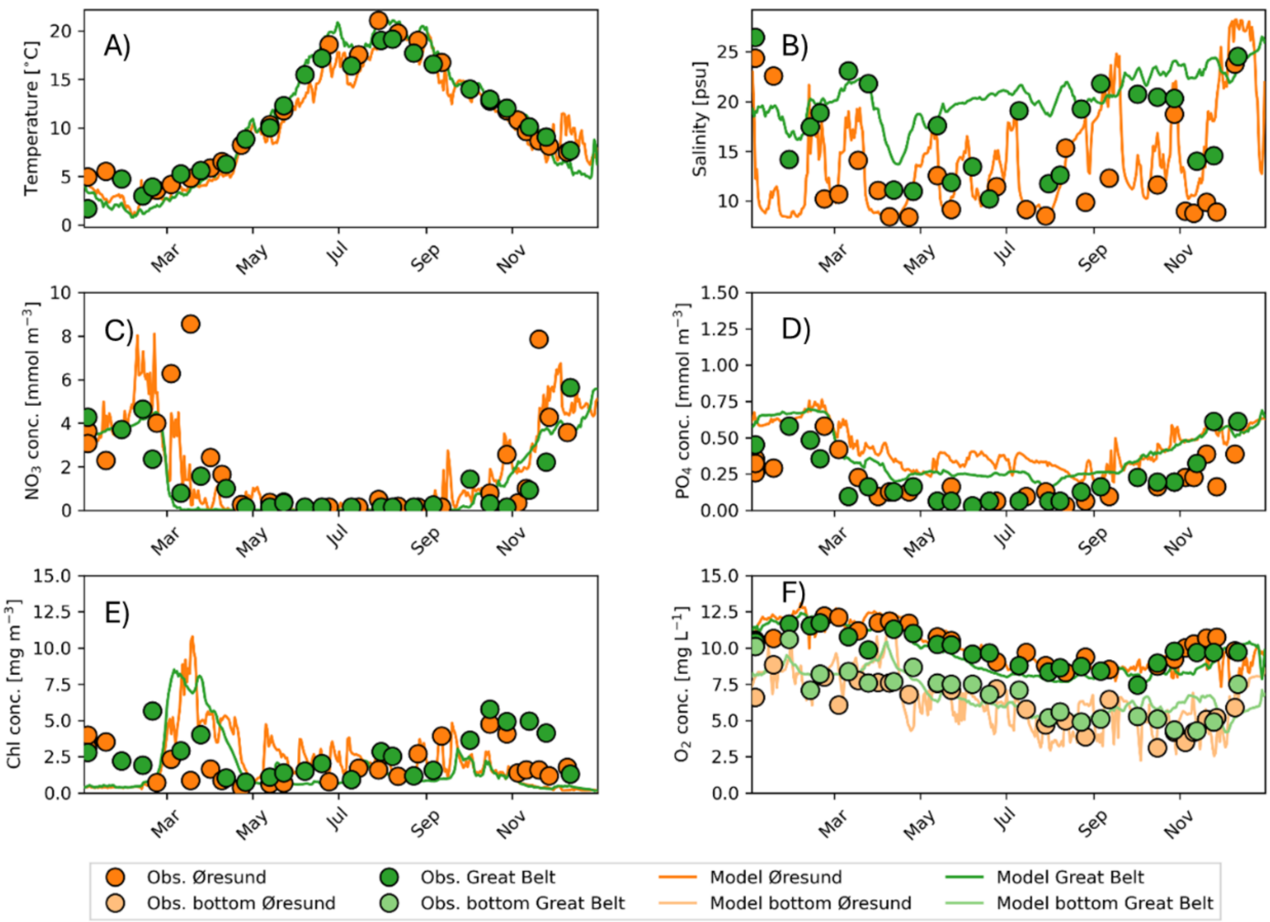

Figure A1.5. Comparison of model results (solid lines) versus monitoring data (points) from the two monitoring stations Great Belt (green) and the Øresund (orange) of A) surface temperature, B) surface salinity, C) surface nitrate concentration, D) surface phosphate concentration, E) surface Chl *a* concentration, and F) surface and bottom oxygen concentration in 2019.

10.5 Inner Danish waters physical and biogeochemical spatial patterns

Model means (April to October) of the physical and biogeochemical variables in REF-NO-FARM are shown in figures A1.6 and A1.7, respectively. Stratification is strongest in the Kattegat and is present in most of the area. Current speeds and bottom stress are highest in the narrow Great Belt and the Sound. Salinity shows a spatial gradient with highest values towards the Kattegat and lowest in the Baltic Sea. Temperature was generally higher in the southern part. Light attenuation was highest next to the freshwater sources along the coastline.

Nutrient and Chl *a* concentrations and zooplankton biomass showed generally highest values in the coastal areas, whereas bottom oxygen and benthos biomass often showed the opposite pattern. Primary- and zooplankton production were depth-integrated 0-40 m and therefore showed high values both along the coastline and in deeper waters of the Danish Straits and southern Kattegat. The simulated patterns are similar to previous model results for the western Baltic Sea (Schrum et al. 2006, Maar et al. 2016).

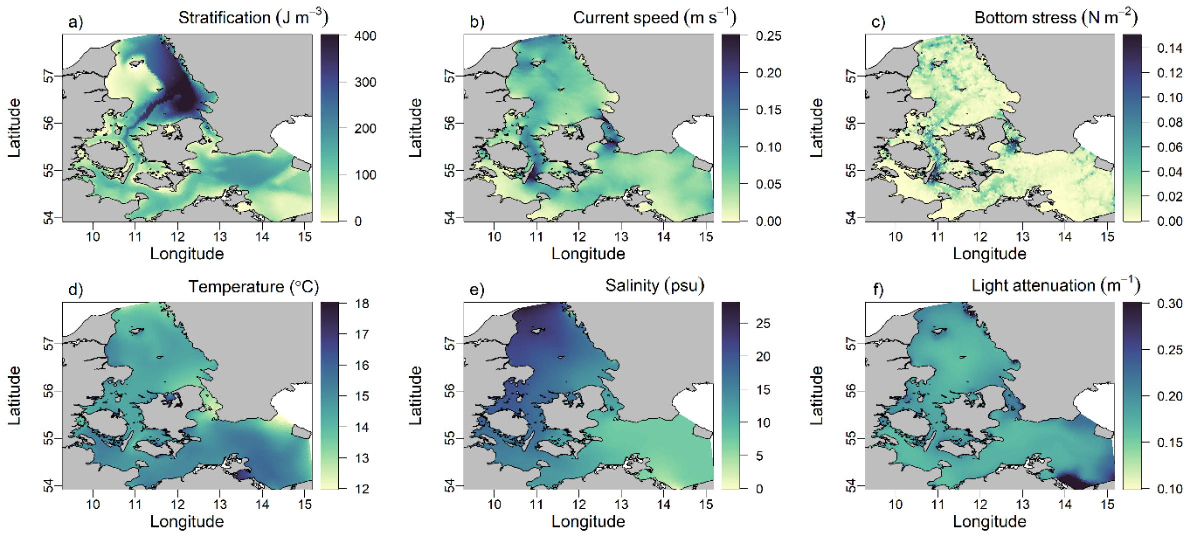

Figure A1.6. Means (April to October 2019) of physical variables, a) stratification index PEA, b) current speed, c) bottom stress, d) temperature, e) salinity, and f) light attenuation for the Inner Danish waters.

10.6 Model quality assurance

The FlexSem model source code is open access and available on zenodo.org (Larsen 2024, Maar et al. 2025) and the FlexSem home page (FlexSem). The hydrodynamic and biogeochemical models have been described and validated in previous publications (Larsen et al. 2020, Maar et al. 2020, Schourup-Kristensen et al. 2024). The implementation of monopile drag was tested in a small-scale set-up before implementation into the regional models (Mohn et al. 2025). The new code was implemented by J. Larsen and quality assured by A. Ishimwe and C. Mohn. The implementation of DON into the Inner Danish water model was based on the documented model from IOW (Neumann et al. 2022). It was implemented by V. Schourup-Kristensen and quality assured by M. Maar. The applied model versions were validated against monitoring data as described in the previous sections.

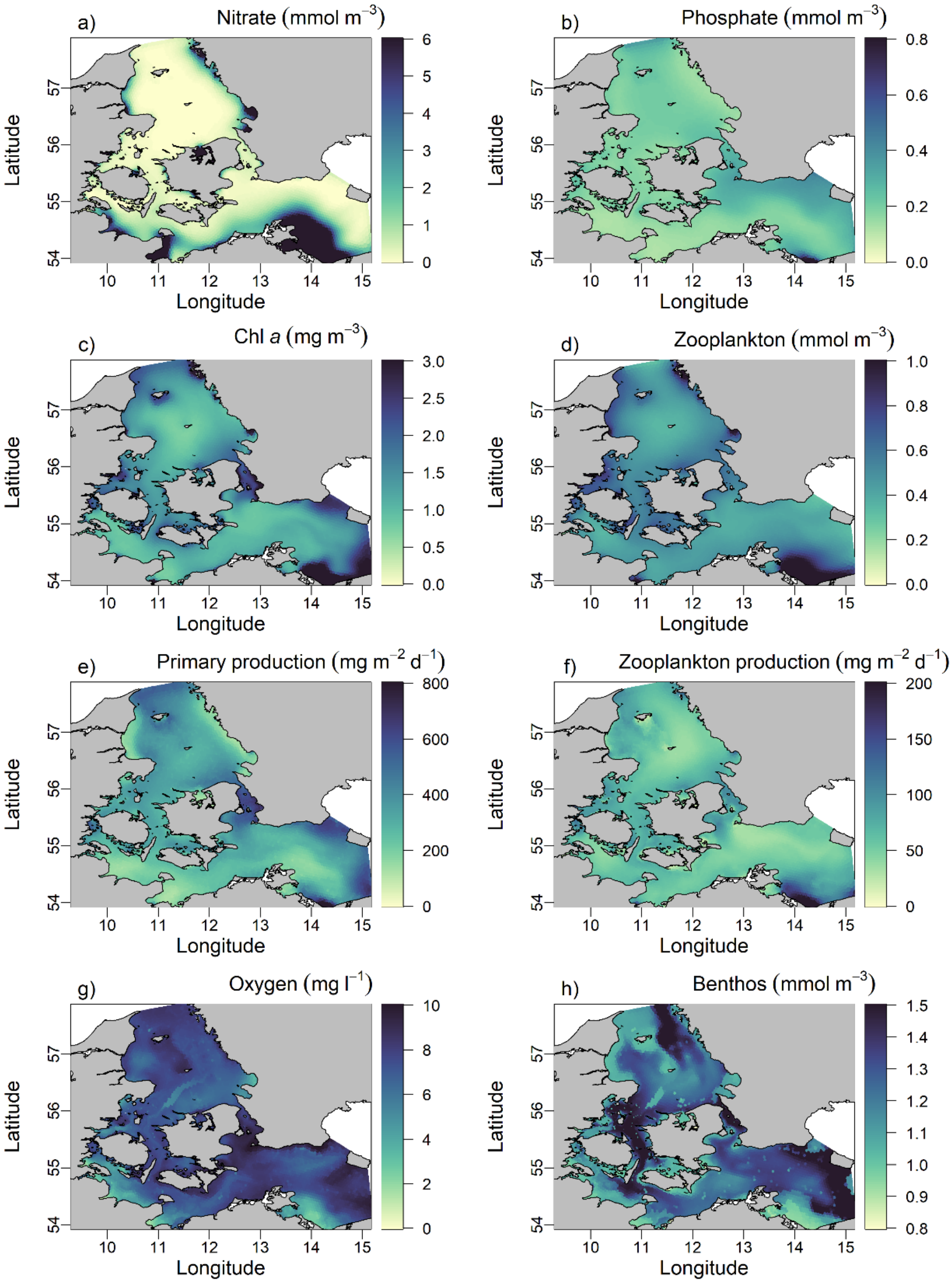

Figure A1.7. Means (April to October 2019) of biogeochemical variables, a) nitrate, b) phosphate, c) Chl a, d) zooplankton, e) primary production, f) zooplankton production, g) oxygen, and h) benthos for the Inner Danish waters.

SPATIAL IMPACTS OF OFFSHORE WIND FARMS ON HYDRODYNAMICS AND BIOGEOCHEMICAL ENVIRONMENT

This report provides a model assessment of the spatial impact of current and future offshore wind development on hydrodynamics and the biogeochemical environment in the North Sea and the Inner Danish waters. Two model scenarios evaluated the impact of i) current distribution (year 2021) and ii) potential future distribution (Year 2030) of offshore wind farms relative to a scenario without wind farms. Stratification decreased in the offshore wind farm areas in the North Sea due to strong monopile mixing. In the Inner Danish waters, stratification increased in a larger area outside the offshore wind farms due to the wind wake effect. Primary production mainly increased in the offshore wind farm areas in the North Sea but decreased outside - although to a lesser degree. In the Inner Danish waters, primary production showed high spatial variability depending on changes in stratification. Overall, there was a slight decrease in primary production for the entire area. The present study shows the importance of including both the wind wake effect and the monopile drag effect since they are opposing forces, making the responses highly complex in space and time in marine waters.

ISBN: 978-87-7156-953-7
ISSN: 2244-9981